2021

Power Scaling of Ice Floe Sizes in the Weddell Sea, Southern Ocean

Tristan J. Coffey
Wright State University

POWER SCALING OF ICE FLOE SIZES IN THE WEDDELL SEA, SOUTHERN OCEAN

A thesis submitted in partial
fulfillment of the requirements for
the degree of Master of Science

by

TRISTAN J. COFFEY

B.A., Wright State University, 2019

2021

Wright State University

Wright State University

Graduate School

April 29, 2021

I hereby recommend that the thesis prepared under my supervision by Tristan J. Coffey entitled Power Scaling of Ice Floe Sizes in the Weddell Sea, Southern Ocean be accepted in partial fulfillment of the requirements for the degree of Master of Science.

Christopher Barton, Ph. D.
Thesis Director

Committee on
Final Examination

Chad Hammerschmidt, Ph. D.
Department Chair

Sarah Tebbens, Ph. D.

Doyle Watts, Ph. D.

Barry Milligan, Ph. D.
Vice Provost for Academic Affairs
Dean of the Graduate School

Abstract

Coffey, Tristan J. M.S. Department of Earth and Environmental Science, Wright State University, 2021. Power Scaling of Ice Floe Sizes in the Weddell Sea, Southern Ocean

The cumulative number versus floe area distribution of seasonal ice floes from four satellite images covering the Summer season (November - February) in the Weddell Sea Antarctica during the summer breakup and melting is fit by two scale-invariant power scaling regimes for the floe areas ranging from 7 to 20 x 10^8 m^2. Scaling exponents, β, for larger floe areas range from -1.5 to -1.7 with an average of -1.6 for floe areas ranging from 6 x 10^6 to 55 x $10^7 m^2$. Scaling exponents, β, for smaller floe areas range from -0.8 to -0.9 with an average of -0.85 for floe areas ranging from 3 x 10^6 to 1.55 x 10^6 m^2. The inflection point between the two scaling regimes ranges from 62 x 10^6 to 151 x 10^6 m^2 and generally moves from larger to smaller floe areas through the summer season. We propose that the two power scaling regimes and the inflection between them are defined during the initial breakup of sea ice solely by the process of fracturing. The distributions of floe size regimes retain their scaling exponents as the floe pack evolves from larger to smaller floe areas from the initial breakup through the summer season, due to scale-independent processes including grinding, crushing, fracture, and melting. The scaling exponents for floe area distribution are in the same range as those reported in previous studies of Antarctic and Arctic floes. A probabilistic model of fragmentation is presented that generates a single power scaling distribution of fragment size.

Table of Contents

List of Figures

List of Tables

Table Number Page

Acknowledgements:

The author would like to thank Greg Geise and Dan Khoel for their help in processing the GIS data and Dr. Christopher C. Barton for helping me select this topic and guiding me through this work. I would like to thank my committee, Dr. Sarah F. Tebbens and Dr. Doyle R. Watts for their constructive contributions to this thesis.

1.0 Introduction

In the winter season (March-October), sea ice forms and floats on the surface of the Southern Ocean (Figure 1) and ranges from 2-3 m thick (smoothed by snow coverage on top, but rough and uneven on the bottom). In November, the ice begins to break up into free floating angular fragments of different shapes and sizes. A floe is defined as a piece of sea ice whose surface area is larger than 1 m^2 (Gherardi, 2015). Newly formed floes in the Southern Ocean, observed in this study and the Arctic Ocean, exhibit rough angular edges, wavy edges, and corners, and in the Southern Ocean range in area from 1 to 20 x 10^8 m^2. Once formed, the floes sizes are reduced by additional fracturing caused by impact, crushing, and grinding into each other due to wave motion, wind, and currents moving under the floe pack and by melting and smoothing along their edges and faces. Larger floes are surrounded by smaller floes which cushion larger floes protecting them from further fracturing, making them less susceptible to fracture by crushing or grinding, suggesting a scale-independent process. In the process of fracturing, only particles of the same size or larger can fracture any given particle (Sammis and King, 2007). This observation is the basis for the probabilistic model put forward in Geise and others, (2016) to explain the power distribution of floe sizes in the Arctic Ocean. The size distribution of floes and their evolution over the Antarctic summer is the subject of this study. This topic is of relevance to marine vessels that encounter floes, to the calculation of sea ice albedo, to the determination of Antarctic heat exchange which is strongly influenced by ice concentrations and the amount of open water between floes (Worby and Allison 1991), and to photosynthetic marine organisms which are dependent upon sunlight penetrating the spaces between floes (Grose and McMinn 2003).

1.1 Calculation of Equivalent Scaling Dimensions

In the literature, the size of ice floes has been approximated on images by either of two methods. The first is by counting the number of pixels in each floe. The second method is the mean caliper diameter method. Each method is illustrated in Figure 2. Power scaling exponents derived from a one-dimensional representation (mean caliper-diameter) of the size of a floe do not have the same values as the power scaling exponents calculated from 2-dimensional flow areas. Stern, Schweiger, Zhang, and Steele (2018) proposed that the scaling exponents can be converted between the mean caliper diameter method and the pixel area method. They propose multiplying the scaling exponent of the area method by two to obtain the scaling exponent of the mean caliper-diameter method but offer no reasoning for this. In contrast, we propose that the scaling exponent of the mean caliper-diameter method be increased by adding one to obtain the scaling exponent derived by the measurement of ice floe area. The basis for our proposal is in Barton and Scholz (1995) which state that the dimensionality of a sampling method sets range of the scaling exponent. For example, a three-dimensional fractal object such as a Menger sponge has a scaling exponent of 2.7. The pattern on a planar cut through a Menger sponge (called a Sierpinski carpet), has a scaling exponent of 1.7, and a one-dimensional sampling (a line) through a Menger sponge has a scaling exponent of 0.7. Therefore, for a one-dimensional sampling strategy, such as the mean caliper-diameter method, a value of one (resulting in a steeper slope on a log-log plot) should be added to the scaling exponent to convert to the scaling exponent of a two-dimensional sampling strategy. In Table 1 I have converted the equivalent area exponent and provided it in parentheses ( ) after each mean caliper-diameter method scaling exponent.

The power scaling exponent of the size distribution of objects also depends on the form of the distribution. Most, but not all, of the power scaling exponents in Table 1 are fit to a cumulative frequency distribution. The remainder of the power scaling exponents is fit to the non-cumulative frequency distribution (histogram). The power scaling exponent of a non-cumulative distribution is an integer (1) less than that of a cumulative distribution of the same data (Burroughs and Tebbens, 2001). Therefore, to calculate a power exponent of a cumulative distribution from a non-cumulative distribution, one needs to add 1 (steeper slope) to the scaling exponent of the non-cumulative distribution.

2.0 Previous Studies

Previous studies plot the cumulative number versus either the floe diameter or the surface area of the floes or the non-cumulative number versus either the floe diameter or the surface area of the floes, both the cumulative number and non-cumulative plots of the data have been fit by a power function with a scaling exponent in the form: $N = Cx^{-\beta}$, where N is the cumulative number of floes greater than x or the number of floes binned over a range of sizes, C is a constant called the activity , and β is the scaling exponent. The mean caliper-diameter method is a one-dimensional measure of a two-dimensional object.

In most studies the floe surface area was approximated by the mean caliper-diameter method where one measures of the distance between parallel calipers tangent to opposite sides of the floe and calculating the mean over all orientations of the calipers (see Figure 2). Note, this is a one-dimensional measure of a two-dimensional object (floe surface area). The mean caliper-diameter method also leads to a different value of the scaling exponent than the grouped pixel area method as discussed above. A few previous studies have used grouped pixel values to approximate the area (a two-dimensional measure) of each floe. To obtain an area of an ice floe using the grouped pixel values method, the same valued pixels are grouped together to form a polygon for the surface of the ice floe and the area is approximated by the number of pixels.

2.1 Southern Ocean

Gherardi and Lagomarsino (2015) analyzed four aerial and satellite images taken in the Weddell Sea during the Spring of 2000, 2001, 2003, and 2009. They grouped white pixels for ice floes and black pixels for water in the images. They calculated the caliper-diameter *d* to represent the area of each floe and found the non-cumulative number versus mean caliper-diameter to be well fit by a single power function with a scaling exponent of -2.0 for mean floe caliper-diameters ranging from 2 to 5000 m.

Lensu (1990) analyzed one image from the Weddell Sea during the summer ice pack break up in February of 1990. Using ice floe areas, she found the cumulative number versus area to be well fit by a single power function with a scaling exponent -1.68 for floes areas ranging from 1 to 350 m^2.

Lu and others (2008) analyzed nineteen aerial photos in the Prydz Bay, East Southern Ocean in December 2004-February 2005 and used the mean caliper-diameter method. The cumulative number vs. mean caliper-diameter was found to be well fit by a single power function with scaling exponents ranging between -0.6 to -1.4 for floe mean caliper-diameters ranging from 2 to 100 m.

Paget and others (2001) analyzed six aerial images in the East Antarctic Sea in August 1995. They used the mean caliper-diameter method. The non-cumulative number vs mean caliper-diameter was found to be well fit by a single power function with scaling exponents ranging from -1.9 to -3.5 for floe mean caliper-diameters ranging from 1 to 150 m.

Steer and others (2008) analyzed 130 aerial images taken in the Weddell Sea, in December 2004. They used the mean caliper-diameter method for mean floe diameters ranging from 2 to 120 m. The non-cumulative number versus mean caliper-diameter is well fit by two scaling exponents. A scaling exponent of -1.9 was found for floes smaller than 20 m and -2.0 to-4.0 for floes larger than 20 m.

Toyota and others (2011) analyzed 122 helicopter images taken in the Weddell Sea, September through October 2006 and 52 in Wilkes Land, September-October 2007. In the Weddell Sea they used the mean caliper-diameter method for floe mean caliper-diameters for floes ranging 2 to 100 m. The cumulative number vs mean caliper-diameter is well fit by two scaling exponents. Scaling exponents from -1.03 to -1.05 were found for floe diameters smaller than 40 m and -5.0 to-5.79 for floe diameters larger than 40 m. In the Wilkes Land they used the mean caliper-diameter method for floe mean caliper-diameters ranging from 2 to 100 m. The cumulative number versus mean caliper-diameter is well fit by two scaling exponents. Scaling exponents from -1.03 to -1.52 were found for floes smaller than 20 to 40 m and -3.15 to-5.51 for floes larger than 20 through 40 m.

Toyota and others (2015) analyzed sixteen helicopter and satellite images taken in Wilkes Land, East Antarctic in September-November 2012. They used the mean caliper-diameter method for mean floe caliper-diameters ranging 5 to 10,000 m. The cumulative number vs diameter is well fit by two scaling exponents. Scaling exponents from -2.9 to –3.1 were found for floe diameters smaller than 100 m and from -1.3 to-1.4 for floe diameters larger than 100 m.

2.2 Arctic Ocean

Geise and others (2016) analyzed six satellite images in the East Siberian Sea from June-August 2000 through 2002. They used pixel counting to measure the floe area. The cumulative number versus diameter is well fit by two power scaling functions with scaling exponents ranging from -0.6 to -1.0 for floe areas ranging from 30 to 28,400,000 m^2.

Gherardi and Lagomarsino (2015) viewed three aerial and satellite images in the Barents Sea during the Spring seasons of 2000, 2001, and 2009. They used the mean caliper-diameter method to measure floe mean caliper-diameters ranging from 2 to 5000 m. The cumulative number vs mean caliper-diameter is well fit by a single power function with a scaling exponent of -2.0.

Holt and Martin (2001) analyzed fifteen satellite images in the Barents and Kara Sea near the Artic Circle during August 1992. They used the mean caliper-diameter method to measure floe mean caliper-diameters   ranging from 1000 to 20,000 m. The cumulative number versus diameter is well fit by a single power function with scaling exponents ranging from -1.9 to -2.6.

Hwang and others (2007) analyzed four satellite images in the Beaufort Sea from May to September 2014. They used the mean caliper-diameter method to measure floe mean caliper-diameters ranging from 450 to 3000 m. The cumulative number versus mean caliper-diameter is well fit by a single power function with scaling exponents ranging from -2.7 to -4.0.

Inoue and others, (2004) analyzed two areal images in the Sea of Okhotsk, February 18, 2000. They used the mean caliper-diameter method to measure floe mean caliper-diameters ranging from 10 to 100 m. The cumulative number versus diameter is well fit by a single power function with scaling exponents ranging from -1.5 to -2.1.

Matsushita (1985) analyzed one satellite image in the Sea of Okhotsk in December 1984. He used the mean caliper-diameter method to measure floe mean caliper-diameters ranging from 5 to 30 m. The cumulative number versus mean caliper-diameter is well fit by a single power function with a scaling exponent of -2.2.

Perovich and Jones (2014) analyzed nine aerial and satellite images in the Beaufort Sea from June to September 1998. They used the mean caliper-diameter method to measure floe mean caliper-diameters ranging from 10 to 10,000 m. The cumulative number versus mean caliper-diameter is well fit by a single power function with scaling exponents ranging from -2.0 to -2.2.

Rothrock and Thorndike (1984) analyzed seven aerial and satellite images in the Beaufort Sea from March to October 1973-1975. They used the mean caliper-diameter method to measure floe mean caliper-diameters ranging from 1000 to 20,000 m. The cumulative number versus diameter is well fit by a single power function with scaling exponents ranging from -1.7 to -2.5.

Stern and others, (2018) analyzed 273 satellite images in the Beaufort and Chukchi Seas from March to October 2013 and 2014. They used the mean caliper-diameter method to measure floe mean caliper-diameters ranging from 10 to 30,000 m. The cumulative number versus diameter is well fit by a single power function with scaling exponents ranging from -2 to -2.9.

Toyota and others, (2006) analyzed four helicopter, icebreaker, and satellite images in the Sea of Okhotsk during February 2003. They used the mean caliper-diameter method to measure floe mean caliper-diameters ranging from 1 to 1500 m. The cumulative number versus diameter is well fit by two scaling exponents. A scaling exponent of -1.15 was found for floes smaller than 40 m and -1.87 for floes larger than 40 m.

Wang and others, (2016) analyzed eighteen satellite images in the Beaufort and Chukchi Seas from Summer to Fall 2014. They used the mean caliper-diameter method to measure floe mean caliper-diameters ranging from 1 to 40,000 m. The cumulative number versus mean caliper diameter is well fit by a single power function with scaling exponents ranging from -2.77 to -4.12.

3.0 Data

This study is based on four mostly cloud free satellite images of four floe packs at different stages of fragmentations during the Antarctic summer months of November 2016, December 2015, January 2015, and February 2015, at different locations in the Weddell Sea (Figure 3) obtained from the USGS (United States Geologic Survey) Earth Explorer (United States Geological Survey, 2016).

The Weddell Sea area was selected because of image clarity, image quality, and cloud coverage of less than twenty percent. The Weddell Sea is a preferred research location for many ice floes studies and is protected by the Antarctic peninsula.

The images used in this study were collected by the Landsat 8 satellite, using the eighth band (panchromatic band). To measure the areas of individual floes, ideally the images should be cloud free because the bands used to image the ice floes do not penetrate through clouds. Melting ponds on the surface of the ice were not removed from the images. Satellite images were greyscaled at 15 m per pixel resolution. In this study, floe area is the measure of floe size in contrast to the mean caliper-diameter as used in most previous studies. A visual inspection of the satellite images reveals no characteristic floes size (e.g., Figures 4, 5, 6, 7, and 8), qualitatively implying that the distribution of floe sizes is scale invariant and might, therefore, be accurately described by a power function.

The satellite tiff files obtained from Earth Explorer were digitized using ESRI's (Environmental Systems Research Institute) geographic information system (GIS) program, ArcPro 2.2. Only floes larger than $3x10^6$ m^2 were included in this study. Tiff pixels were classified into two classes: ice and water, using ArcPro's Supervised Classification tool. The tiff pixels were split into two classes, the high brightness pixels represented the ice, while the low brightness pixels represented water. Individual floes were identified by the grouping of ice class pixels surrounded by water class pixels. The Raster to Polygon tool in ArcPro 2.2 was used to automatically identify the edges of each floe. The resulting floe polygons formed the floes as seen in the raster image. The area and perimeter of each floe in the raster image, were automatically tabulated in the attribute table by ArcPro 2.2. Floes cut off by the outer edge of the image were excluded from this study.

4.0 Analysis

A plot of the cumulative number vs. floe area is shown in Figure 9. The data for each image is well fit by two power functions, with an inflection point between them, each of the form $N = Cx^{-\beta}$, where N is the number of floes with an area greater than x, C is a constant of proportionality and a measure of the activity, and β is the scaling exponent or fractal dimension (Barton,1995). For each distribution, we find the parameters C and β using the Levenberg-Marquardt algorithm to minimize Chi-squared (Press et al. 2001) using the Wavemetrics software IgorPro version 6.37. This method is appropriate for fitting the power functions to data and calculating the associated error; the method assumes that the errors in fitting the functions to the data are normally distributed (Press et al. 2001). In all analyses, the data were fit by the power function $y_0+Cx^{-\beta}$, where y_0 was set to 0 and the fit was found to converge. Errors are reported to plus/minus on standard deviation in Table 1.

Each of the four data sets analyzed and plotted on Figure 9 exhibit two power scaling regimes where larger floes have a distribution whose scaling exponent is greater than that of the small floes. The scaling exponents, β, exhibit a range of values (Table 1). The scaling region for smaller floes has scaling exponents β ranging from -0.8 to -0.9. The larger floes have scaling exponents β ranging from -1.5 to -1.7. The inflection points between the two regions ranges from 62×10^6 to 151×10^6 m^2. The number of floes analyzed in each image ranges from 303 to 1078 (Table 1).

Inflection points decrease sequentially from November to February as sea ice evolves from larger to smaller floes throughout the season due to grinding, crushing, fracturing, and melting as seen in Figure 4b.

Summing the areas of the larger floes above the inflection point and dividing by the total floe area for each image indicates that the area of the large floes is 22-44 % of the total floe area (Table 1). Note that this is the opposite found in the Arctic by Geise, Barton, and Tebbens, 2017 where the larger floes, those greater than the inflection points accounted for 90+ percent of the total floe area.

5.0 Fragmentation

Geise, Barton, and Tebbens, 2016 proposed a model that produces a power cumulative frequency versus the size of fragments. which may explain the power distribution of floe areas but not an inflection point between the larger and smaller floe size distributions. Figure 10 illustrates their probabilistic model for fragmentation of a cubic volume for any material where the fracture is the method of fragmentation. At iteration n = 1 the volume is broken into eight smaller cubes of equal size. At iteration n = 2 some of the eight cubes are randomly selected and broken into eight smaller cubes. At iteration n = 3 the model bifurcates based on whether (A) only the smallest of the cubes or (B) a cube of any size, can be randomly selected and broken. With many iterations, the rule for A or B determines the cumulative frequency versus size distribution of the fragments. Rule A leads to a power fragment size distribution and Rule B leads a lognormal fragment size distribution. Power distributions are observed in the size (area) of floes, it follows that a process following Rule A is appropriate for ice floes. Sammis and King (2007) propose a physical process that results in power scaling of fragmentation sizes in geologic materials such as fault gauge (see Table 1 in Geise and others, 2016 for examples of power fragment sizes in geologic materials). In their proposed process, adjacent fragments must be approximately the same size to break by fracture. The authors observe that in the process of fragmentation by grinding and crushing, larger fragments become surrounded by smaller fragments that cushion them and protected them from further fracturing thus greatly reducing the probability of further fragmentation. Furthermore the authors propose that such a process occurs simultaneously over a broad range of length scales leading to a power distribution in fragmentation size observed in many brittle materials under a wide range of conditions. Visual inspection of Figures 3a, 4a, 5, and 6 reveal that for ice floes the large fragments are surrounded by smaller fragments which may similarly have cushioned them and reduced the probability of further fragmentation.

6.0 Discussion and Conclusions

The distribution of floe areas in each image is well fit by two power functions that meet at an inflection point between the larger floes and the smaller floes, Figure 9. The floe areas larger than the inflection points range from (6 x 10^6 to 55 x $10^7 m^2$) are well fit by a power function with scaling exponents ranging from -1.5 to -1.7) while the floes areas smaller than the inflection points range from 3 x 10^6 to 1.55 x 10^6 m^2 are well fit by a power function with scaling exponents ranging from -0.8 to -0.9. The inflection points range from 62 x 10^6 to 151 x 10^6 m^2.

This study supports previous studies that found that the cumulative number versus floe area distribution of seasonal ice floe areas in the Antarctic region are distributed in two power scaling regimes. This is also the result found by (Geise and others, 2016) for the distribution of ice floe areas in the Arctic. We suggest that the two power scaling regimes and the inflection between the large and small floes are established during the initial breakup of the sea ice solely by the process of fracture. The distributions of floe size regimes retain their scaling exponent as the sea ice evolves from larger to smaller floes throughout the season due to grinding, crushing, fracture, and melting as seen in Figure 4b. Figure 10 shows a probabilistic model for fragmentation by breaking a cubic volume by fracturing by two different rules (Geise and others, 2016). To break a floe of a given size by fracture into one or more pieces requires impact with a floe of approximately the same or greater size. Sammis and King (2007) observed that during the process of fragmentation by grinding, crushing, and fracture, fragments of any size that become surrounded and cushioned by smaller fragments and tended not to be broken down further. This same process could protect larger floes from further fragmentation (Figure 3b). The study infers that this cushioning process leads to a power distribution in fragmentation size.

This study leaves several fundamental questions unanswered. First is why do larger floes and smaller floes exhibit different scaling exponents? The second is why are the inflection points located at the floe sizes where they are observed? The change in scaling exponent and inflection points are not observed in other materials. What makes the fracturing of ice different from fracturing of all other materials? Can a model of fracturing be constructed that exhibits an inflection point? Answers to these questions are necessary to understand the fracturing process that results in the distribution of ice floe areas.

References

Altshiller-Court, N., 2007, College geometry: an introduction to the modern geometry of the triangle and the circle. Mineola: Dover Publications.

Barton, C. C., 1995, Fractal analysis of the scaling and spatial clustering of fractures in rock. In C. C. Barton and P. R. La Pointe (Eds.), Fractals in the earth sciences p. 141–177. New York: Plenum Press.

Barton, C.C., and Scholz, C.H., 1995, The fractal size and spatial distribution of hydrocarbons: in Barton, C.C., and La Pointe, P.R., eds., Fractals in Petroleum Geology and Earth Processes: Plenum Press, New York, p. 13-33.

Burroughs, S., Tebbens, S., 2001, Upper-truncated Power Laws in Natural Systems, Pure Appl. Geophys. 158, p. 741–757. https://doi.org/10.1007/PL00001202

Geise, G.R., Barton, C.C. and Tebbens, S.F., 2016, Power Scaling and Seasonal Changes of flow areas in the Arctic East Siberian Sea, Pure Applied Geophysics., 174: 387. http://doi.org/10.1007/s00024-016-1364-2

Gherardi, M., and Lagomarsino, M. C., 2015, Characterizing the size and shape of sea ice floes. Scientific Reports, 5, 10226. doi:10.1038/srep10226

Grose, M., and McMinn, A., 2003, Algal biomass in East Antarctic Pack ice: How much is in the East? Antarctic biology in a global context, In the Proceedings of the VIIIth SCAR International Biology Symposium, August 27–September 1, 2001, Vrije Universiteit, Amsterdam, The Netherlands, p. 182–186

Herman, A., 2010, Sea-ice floe-size distribution in the context of spontaneous scaling emergence in stochastic systems. Physical Review E, 81, 066123-1–066123-5.

Inoue, J., Wakatsuchi, M., and Fujiyoshi, Y., 2004, Ice floe distribution in the Sea of Okhotsk in the period when sea-ice extent is advancing, Geophysical Research Letters, 31(20), L20303. doi:10.1029/2004GL020809.

Lu, P., Li, Z.J., Zhang, Z.H. and Dong, X.L., 2008, Aerial observations of floe size distribution in the marginal ice zone of summer Prydz Bay. Journal Geophysical Research: Oceans. Vol. 113, Issue C2. DOI: 10.1029/2006JC003965

Lensu, M., 1990, The fractality of sea ice cover. Finnish Institute of Marine Research: Ice Symposium, Espoo, Finland, p. 300–313.

Mandelbrot, B.B., 1982, The Fractal Geometry of Nature, W.H. Freeman and Co, San Francisco, 461p.

National Aeronautics and Space Administration, 2016, https://earthobservatory.nasa.gov/features/SeaIce/page4.php

Paget, M.J., Worby, A.P. and Michael, KJ., 2001, Determining the floe-size distribution of East Antarctica sea ice from digital aerial photographs. Annals of Glaciology Vol. 33, p. 94–100. DOI: 10.3189/172756401781818473

Press, W. H., Teukolsky, S. A., Vetterling, W. T., and Flannery, B. P., 2001, Numerical recipes in FORTRAN: the art of scientific computing, Cambridge University Press, 1195p.

Sammis, C. G., and King, G. C. P., 2007, Mechanical origin of power law scaling in fault zone rock. Geophysical Research Letters, 34, L04312. doi:10.1029/2006GL028548.

Steer, A., Worby, A., and Heil, P., 2008, Observed changes in sea-ice floe size distribution during early summer in the western Weddell Sea, Deep-Sea Research II,vol. 55, p. 933–942. DOI: 10.1016/j.dsr2.2007.12.016

Stern, H.L., Schweiger, A. J., Stark, M., Zanj, J., Steele, M., Hwang, B., 2018, Seasonal evolution of the sea-ice floe size distribution in the Beaufort and Chukchi seas. Elementa Science of the Anthropocene, 6: 48. DOI: https://doi.org/10.1525/elementa.305

Toyota, T, Haas, C and Tamura, T., 2011, Size distribution and shape properties of relatively small sea-ice floes in the Antarctic marginal ice zone in late winter. Deep-Sea Res II Vol. 58, p. 1182–1193. DOI: 10.1016/j.dsr2.2010.10.034

Toyota, T, Kohout, A and Fraser, A., 2015, Formation processes of sea ice floe size distribution in the interior pack and its relationship to the marginal ice zone off East Antarctica. Deep Sea Research Part II Topical Studies in Oceanography, Vol. 131, p. 28-40, https://doi.org/10.1016/j.dsr2.2015.10.003

United States Geological Survey (USGS), 2016, Earth Explore, https://earthexplorer.usgs.gov/

Zhang, Q., and Skjetne, R., 2018, Sea Ice Image Processing with MATLAB, CRC Press, Boca Raton, FL, 272p.

Appendix: Listing of ice floe areas measured for each of the four satellite images.

Month	ID Number	Area m^2	Month	ID Number	Area m^2	Month	ID Number	Area m^2	Month	ID Number	Area m^2
Nov	1	544815900	Dec	1	344319230	Jan	1	343484383	Feb	1	389903965
	2	500292000		2	338008713		2	311788822		2	343848837
	3	276590700		3	314906711		3	261862141		3	218520047
	4	273765600		4	281214728		4	256253434		4	138313812
	5	213774300		5	269676898		5	250418253		5	130855175
	6	207762300		6	267961671		6	213804484		6	122139901
	7	194832900		7	267056997		7	168619777		7	110196933
	8	193618800		8	266922588		8	161722406		8	107029098
	9	187589700		9	238486384		9	158920251		9	104439238
	10	173933100		10	235311595		10	146293264		10	100422274
	11	161494200		11	231756154		11	145108255		11	91672364
	12	155881800		12	217474192		12	129161842		12	91217766
	13	150412500		13	200989469		13	109376761		13	90588602
	14	143724600		14	196498470		14	108150532		14	90059376
	15	125994600		15	186417703		15	95068211		15	86078807
	16	124919100		16	182755304		16	92419465		16	85337635
	17	122048100		17	173405684		17	92147070		17	74345640
	18	113325300		18	169137174		18	88997363		18	72629833
	19	111249000		19	161500772		19	87604186		19	70131218
	20	110777400		20	154967341		20	87360852		20	68514877
	21	109008000		21	151948489		21	85035166		21	68229710
	22	104685300		22	151382282		22	84702406		22	65328224
	23	94549500		23	150899489		23	80018420		23	58916610
	24	91449000		24	143255950		24	76296826		24	58110111
	25	89371800		25	131349734		25	76082745		25	57512812
	26	88679700		26	125344815		26	75880063		26	48580197
	27	87755400		27	123098138		27	75784204		27	47678374
	28	87318000		28	122283860		28	75444298		28	46420868
	29	81079200		29	119090349		29	74287113		29	45872144
	30	77159700		30	117805988		30	74064132		30	45275582
	31	76784400		31	117334863		31	72551103		31	44727364
	32	76001400		32	116337297		32	71949981		32	42745284
	33	73890900		33	112323039		33	70414696		33	41461061
	34	72901800		34	110674171		34	68781857		34	40682526
	35	71992800		35	110086445		35	68442335		35	38929306
	36	71452800		36	104415448		36	66680622		36	38043543
	37	69929100		37	100239530		37	65059662		37	37952524
	38	68607900		38	99354957		38	63402780		38	37342146
	39	68015700		39	97301695		39	62084638		39	37154607
	40	65193300		40	92563624		40	61257045		40	34041489
	41	64486800		41	88867164		41	60190499		41	33949698
	42	59382900		42	87733899		42	59919493		42	33354148
	43	59040900		43	83829895		43	59585949		43	33140887
	44	58407300		44	82847810		44	58810659		44	31634932
	45	55800000		45	82840505		45	58548024		45	30802585
	46	55089000		46	80248883		46	55332986		46	30451671
	47	54007200		47	80074036		47	54797148		47	30265437
	48	53569800		48	77734774		48	53956463		48	30092983
	49	51939000		49	77363670		49	53929737		49	29515827
	50	51475500		50	76835597		50	53399910		50	28956969
	51	51038100		51	75635068		51	53349991		51	28809079
	52	49725000		52	74120406		52	51960898		52	28663315
	53	47368800		53	72693329		53	51897626		53	28455239
	54	47349000		54	70145520		54	49270470		54	28378527
	55	44604000		55	69748160		55	48562365		55	27650014
	56	44205300		56	64307768		56	47905339		56	27290357
	57	43796700		57	61708946		57	47380132		57	26590599
	58	43285500		58	61642504		58	47218762		58	26232453
	59	43193700		59	61364808		59	46101949		59	25977543
	60	41644800		60	59382035		60	46098388		60	25796268
	61	41440500		61	57271090		61	45183746		61	25308987
	62	40829400		62	56984744		62	44257770		62	24841309
	63	38412900		63	56072110		63	44197212		63	24733948
	64	36951300		64	55331099		64	44060109		64	24276400
	65	35621100		65	55124652		65	43422483		65	23574084
	66	34621200		66	54913093		66	42612877		66	23234658
	67	34214400		67	52540762		67	42168786		67	23201323
	68	34035300		68	51525169		68	41611775		68	23191772
	69	32900400		69	51257180		69	41368171		69	22935875
	70	32782500		70	51025236		70	40820155		70	22900975
	71	32779800		71	50757207		71	40545641		71	22314381
	72	31950000		72	50463844		72	39988551		72	21354790
	73	31667400		73	49577467		73	39893025		73	20660482
	74	31419900		74	49059865		74	39677143		74	20507779
	75	31022100		75	48181809		75	39345963		75	20335716
	76	30977100		76	47891745		76	39342237		76	20061485
	77	30966300		77	47311174		77	39248837		77	19782912
	78	30722400		78	47285531		78	37990405		78	19757397
	79	30448800		79	47051998		79	37476992		79	19379388
	80	29480400		80	46697169		80	37250422		80	19332630
	81	29052000		81	46544095		81	36028423		81	19095987
	82	28341000		82	46535666		82	35699410		82	19025415

83	27695700	83	46048319	83	35169771	83	18823001
84	27691200	84	45957206	84	33988232	84	18719945
85	27005400	85	45594309	85	33877742	85	18520960
86	26788500	86	45486186	86	32770382	86	18472513
87	26660700	87	45241100	87	32330330	87	18412203
88	26633700	88	45165654	88	31292937	88	18002402
89	26507700	89	44828458	89	31234443	89	17430100
90	25659900	90	44715366	90	30973514	90	17304203
91	25144200	91	44587322	91	30868055	91	17277785
92	25137000	92	44501750	92	30867102	92	16647844
93	24825600	93	44364159	93	30232127	93	16505543
94	24281100	94	44223814	94	29262980	94	16439390
95	24102000	95	42955723	95	29201551	95	16027975
96	23474700	96	42446862	96	29193854	96	15944130
97	23238000	97	42324953	97	29138896	97	15930116
98	23066100	98	41890170	98	29081769	98	15869352
99	22925700	99	41438617	99	28653304	99	15643856
100	22682700	100	41362671	100	28517761	100	15595284
101	22584600	101	41218318	101	28386384	101	14934611
102	22494600	102	41114879	102	27773333	102	14865023
103	22207500	103	40884251	103	27606467	103	14777306
104	22169700	104	39852483	104	27047360	104	14723724
105	21659400	105	39828080	105	26785290	105	14478018
106	21580200	106	39196078	106	26732672	106	14256855
107	21366000	107	39190149	107	26607643	107	13763310
108	21249900	108	39112412	108	26432297	108	13709411
109	21232800	109	38551318	109	26396438	109	13515999
110	21188700	110	38461060	110	26155377	110	13504743
111	20779200	111	38333524	111	26061717	111	13073662
112	20753100	112	38218972	112	25971754	112	13038377
113	20526300	113	38218403	113	25622701	113	12957302
114	20517300	114	38039739	114	25475395	114	12774410
115	20456100	115	37991763	115	25348898	115	12743370
116	20371500	116	37526405	116	25289963	116	12719633
117	20275200	117	37468751	117	25232273	117	12687380
118	20241900	118	36924616	118	24509545	118	12684885
119	20092500	119	36665776	119	24277153	119	12619045
120	19677600	120	36083765	120	24242845	120	12492163
121	19187100	121	35856509	121	23620059	121	12441538
122	19130400	122	35761365	122	23479424	122	12375370
123	18999900	123	35502600	123	23464890	123	12088224
124	18534600	124	35064621	124	23428660	124	11742525
125	18431100	125	34937237	125	22595344	125	11368312
126	18405900	126	34670707	126	22588848	126	11318436
127	18395100	127	34431371	127	22289894	127	10970713
128	18199800	128	33939910	128	22126476	128	10898786
129	17992800	129	33818552	129	21886179	129	10894968
130	17955000	130	33426288	130	21866333	130	10701251
131	17824500	131	33419931	131	21672746	131	10647812
132	17784000	132	32967205	132	21379346	132	10576135
133	17268300	133	32135054	133	21295913	133	10515863
134	17249400	134	31993022	134	20986167	134	10342741
135	17093700	135	31864006	135	20713944	135	10232799
136	16773300	136	31807695	136	20685860	136	10136441
137	16706700	137	31399973	137	20429949	137	10038897
138	16656300	138	31197519	138	19908367	138	9664001
139	16626600	139	31065999	139	19887658	139	9640967
140	16537500	140	31056555	140	19856082	140	9624636
141	16406100	141	30621884	141	19642992	141	9418416
142	16344900	142	29580408	142	19571552	142	9158229
143	16267500	143	29483073	143	19348911	143	8968872
144	16191900	144	29455514	144	19316049	144	8901220
145	16126200	145	29446494	145	19268011	145	8863088
146	15918300	146	29347310	146	19198486	146	8856103
147	15858000	147	29270736	147	19157015	147	8794614
148	15724800	148	28998664	148	19119778	148	8749162
149	15598800	149	28711509	149	19005753	149	8748577
150	15567300	150	28527846	150	18900355	150	8684426
151	15487200	151	28400090	151	18892802	151	8661550
152	15453000	152	28284829	152	18623507	152	8644266
153	15169500	153	27857457	153	18416284	153	8625641
154	15078600	154	27644470	154	18392728	154	8556106
155	14766300	155	27377781	155	18271732	155	8530431
156	14671800	156	27277537	156	18078802	156	8394924
157	14574600	157	27212284	157	18067343	157	8386394
158	14526000	158	27177137	158	17694993	158	8330113
159	14515200	159	27142307	159	17545566	159	8326488
160	14358600	160	27131813	160	17513540	160	8298818
161	14216400	161	27091397	161	17334553	161	8153830
162	14184900	162	27075185	162	17223898	162	8127482
163	14103000	163	26886069	163	17198160	163	8062310
164	13961700	164	26378271	164	17161695	164	7822049
165	13901400	165	26330011	165	17123498	165	7458716

166	13629600	166	26288818	166	17024716	166	7438681
167	13557600	167	26197053	167	16966456	167	7296341
168	13508100	168	26010348	168	16816708	168	7208512
169	13441500	169	25999574	169	16776016	169	7131292
170	13287600	170	25883219	170	16739053	170	7129082
171	13129200	171	25798019	171	16694444	171	7085775
172	13101300	172	25568485	172	16625492	172	7085412
173	13054500	173	25479553	173	16614923	173	7068400
174	13029300	174	25438387	174	16514770	174	7006619
175	12921300	175	25308072	175	16487538	175	6875926
176	12580200	176	25196425	176	16433307	176	6768484
177	12426300	177	24845117	177	16313483	177	6641648
178	12403800	178	24757911	178	16307428	178	6443163
179	12303900	179	24687208	179	16302233	179	6389465
180	12273300	180	24568513	180	16213218	180	6366492
181	12242700	181	24538091	181	16161513	181	6298820
182	12232800	182	24512965	182	16026230	182	6292382
183	12231900	183	24214636	183	15723516	183	6141741
184	12203100	184	24019890	184	15417559	184	6111971
185	12122100	185	23820032	185	15177121	185	6050872
186	12114000	186	23735072	186	15139943	186	5957861
187	12059100	187	23663868	187	15090098	187	5956455
188	12000600	188	23464248	188	15056523	188	5925642
189	11948400	189	23259979	189	15054723	189	5916634
190	11935800	190	23205292	190	15037049	190	5894979
191	11934900	191	22702225	191	15022911	191	5846767
192	11934000	192	22650476	192	15015169	192	5844272
193	11871000	193	22262997	193	14909968	193	5750424
194	11669400	194	22119160	194	14899036	194	5736546
195	11636100	195	22106691	195	14843569	195	5697307
196	11506500	196	21851070	196	14696149	196	5665695
197	11481300	197	21759927	197	14611535	197	5625699
198	11353500	198	21703309	198	14604269	198	5624581
199	11351700	199	21418663	199	14561624	199	5618575
200	11318400	200	21321476	200	14558444	200	5591896
201	11279700	201	21219905	201	14455547	201	5562977
202	11276100	202	21063006	202	14306400	202	5501975
203	11065500	203	20986017	203	14272649	203	5400202
204	10904400	204	20810238	204	14238741	204	5257939
205	10879200	205	20600929	205	14209523	205	5244906
206	10823400	206	20532545	206	14173319	206	5240950
207	10730700	207	20329007	207	14110166	207	5214187
208	10661400	208	20323787	208	14090002	208	4975367
209	10639800	209	20229632	209	13770827	209	4880047
210	10512000	210	20031050	210	13578971	210	4821630
211	10482300	211	20002220	211	13526727	211	4699416
212	10452600	212	19746593	212	13399688	212	4664715
213	10448100	213	19727798	213	13315217	213	4580608
214	10409400	214	19704472	214	13280843	214	4536514
215	10359000	215	19624306	215	13242896	215	4534242
216	10321200	216	19619810	216	13225067	216	4527819
217	10308600	217	19601122	217	13193276	217	4509749
218	10241100	218	19514251	218	13095836	218	4459170
219	10233900	219	19444356	219	13016296	219	4445309
220	10198800	220	19397820	220	12956385	220	4438937
221	10189800	221	19366789	221	12948742	221	4432392
222	10113300	222	18847881	222	12917570	222	4420886
223	10006200	223	18778035	223	12912965	223	4411103
224	9899100	224	18739013	224	12884664	224	4385642
225	9821700	225	18637995	225	12862233	225	4378205
226	9806400	226	18633385	226	12855509	226	4270137
227	9734400	227	18592903	227	12806798	227	4267783
228	9734400	228	18422895	228	12788424	228	4261676
229	9665100	229	18345380	229	12738691	229	4253460
230	9664200	230	18248050	230	12723716	230	4248621
231	9584100	231	18181579	231	12668044	231	4226128
232	9573300	232	18133230	232	12663232	232	4184614
233	9491400	233	18120184	233	12644849	233	4167494
234	9471600	234	18087178	234	12533117	234	4167028
235	9450900	235	17990170	235	12436240	235	4144399
236	9421200	236	17989940	236	12328524	236	4144270
237	9342900	237	17928027	237	12262025	237	4132213
238	9264600	238	17913434	238	12194325	238	4130567
239	9175500	239	17785185	239	12072979	239	4107033
240	9120600	240	17674571	240	12072582	240	4076357
241	9079200	241	17667404	241	11929364	241	4070174
242	8964900	242	17646263	242	11900698	242	4066156
243	8928900	243	17618530	243	11897799	243	4035704
244	8897400	244	17562828	244	11879729	244	4021288
245	8847900	245	17516938	245	11852759	245	4010397
246	8827200	246	17486454	246	11827937	246	3944375
247	8710200	247	17336818	247	11751364	247	3898874
248	8691300	248	17305812	248	11750445	248	3895312
249	8666100	249	17286487	249	11741332	249	3844777

249	8666100	249	17286487	249	11741332	249	3844777
250	8659800	250	17226066	250	11651811	250	3839902
251	8658900	251	17163989	251	11634551	251	3799978
252	8658900	252	17097966	252	11547588	252	3785855
253	8611200	253	17046211	253	11545539	253	3784865
254	8546400	254	16977414	254	11498716	254	3779418
255	8545500	255	16966417	255	11475667	255	3771535
256	8520300	256	16862915	256	11421030	256	3737889
257	8440200	257	16823649	257	11395619	257	3728818
258	8426700	258	16755650	258	11349165	258	3727311
259	8397900	259	16694418	259	11324383	259	3708153
260	8394300	260	16399668	260	11253877	260	3691343
261	8392500	261	16328475	261	11222075	261	3652846
262	8345700	262	16327670	262	11203779	262	3645492
263	8343000	263	16230292	263	11202840	263	3557697
264	8326800	264	16179256	264	11134795	264	3449219
265	8298000	265	16089819	265	10922786	265	3005628
266	8237700	266	16003521	266	10867267		
267	8203500	267	15980114	267	10853943		
268	8169300	268	15890326	268	10789680		
269	8145000	269	15863037	269	10762199		
270	8091900	270	15844043	270	10678130		
271	8009100	271	15763991	271	10635365		
272	8004600	272	15678674	272	10622303		
273	7988400	273	15657003	273	10589027		
274	7936200	274	15582565	274	10558801		
275	7875900	275	15509027	275	10483276		
276	7802100	276	15482258	276	10470791		
277	7792200	277	15438927	277	10409729		
278	7767000	278	15426593	278	10376984		
279	7750800	279	15403402	279	10358943		
280	7740900	280	15396230	280	10358040		
281	7670700	281	15369603	281	10300652		
282	7632900	282	15297463	282	10299293		
283	7545600	283	15141845	283	10267142		
284	7542900	284	15136481	284	10264747		
285	7533000	285	15117922	285	10264488		
286	7488900	286	15038812	286	10263910		
287	7465500	287	15036899	287	10223989		
288	7464600	288	14866111	288	10197390		
289	7435800	289	14858130	289	10151257		
290	7400700	290	14828392	290	10123681		
291	7367400	291	14789047	291	10121630		
292	7349400	292	14785510	292	10100414		
293	7346700	293	14491972	293	10047382		
294	7341300	294	14463851	294	10044431		
295	7340400	295	14372923	295	10039263		
296	7310700	296	14340763	296	9989022		
297	7263900	297	14314392	297	9956074		
298	7247700	298	14312635	298	9943492		
299	7197300	299	14263695	299	9941284		
300	7182000	300	14183252	300	9909826		
301	7177500	301	14181113	301	9884829		
302	7166700	302	14174349	302	9766292		
303	7146000	303	14117451	303	9721028		
304	7025400	304	13858522	304	9711037		
305	6996600	305	13844956	305	9679801		
306	6961500	306	13792895	306	9583370		
307	6953400	307	13792767	307	9545267		
308	6939900	308	13750843	308	9525236		
309	6903000	309	13716617	309	9476907		
310	6891300	310	13699948	310	9457304		
311	6822900	311	13624309	311	9443028		
312	6821100	312	13587313	312	9436944		
313	6811200	313	13563494	313	9404674		
314	6794100	314	13481986	314	9385541		
315	6778800	315	13472235	315	9336377		
316	6750000	316	13421773	316	9301693		
317	6743700	317	13360191	317	9300083		
318	6707700	318	13357235	318	9159932		
319	6703200	319	13336057	319	9132137		
320	6674400	320	13323203	320	9079784		
321	6653700	321	13295977	321	9073864		
322	6638400	322	13259798	322	9040777		
323	6636600	323	13153997	323	8997265		
324	6600600	324	13071726	324	8986869		
325	6594300	325	13047208	325	8896159		
326	6502500	326	12976425	326	8879097		
327	6486300	327	12938728	327	8878908		
328	6483600	328	12936648	328	8875339		
329	6460200	329	12848871	329	8838078		
330	6453900	330	12825301	330	8753380		

331	6436800	331	12815966	331	8692599
332	6396300	332	12792492	332	8666073
333	6389100	333	12751368	333	8665641
334	6379200	334	12671319	334	8642055
335	6227100	335	12669125	335	8637493
336	6222600	336	12654813	336	8619961
337	6219900	337	12632566	337	8614190
338	6157800	338	12624377	338	8608120
339	6138000	339	12610346	339	8600144
340	6138000	340	12581973	340	8586339
341	6096600	341	12563867	341	8567193
342	6054300	342	12539687	342	8554868
343	6023700	343	12527826	343	8445142
344	5971500	344	12453947	344	8424647
345	5933700	345	12444456	345	8371334
346	5910300	346	12442674	346	8328897
347	5909400	347	12402781	347	8272912
348	5898600	348	12371351	348	8250110
349	5895900	349	12350915	349	8198979
350	5884200	350	12341130	350	8187853
351	5875200	351	12338016	351	8177391
352	5858100	352	12325693	352	8174618
353	5833800	353	12315132	353	8162327
354	5819400	354	12287994	354	8152351
355	5814900	355	12285669	355	8145999
356	5810400	356	12217924	356	8142977
357	5802300	357	12186470	357	8122949
358	5770800	358	12161556	358	8108211
359	5767200	359	12152411	359	8099607
360	5763600	360	12126019	360	8014823
361	5702400	361	12117703	361	7988432
362	5679000	362	12108681	362	7983631
363	5667300	363	12105944	363	7959361
364	5653800	364	12052439	364	7877985
365	5640300	365	12032006	365	7855151
366	5639400	366	12022893	366	7829649
367	5637600	367	11907097	367	7799436
368	5605200	368	11905273	368	7715059
369	5598900	369	11804635	369	7703827
370	5598000	370	11768621	370	7692391
371	5575500	371	11751912	371	7666862
372	5562900	372	11733730	372	7641565
373	5548500	373	11708835	373	7624551
374	5522400	374	11679458	374	7556033
375	5494500	375	11661935	375	7528560
376	5487300	376	11654782	376	7517777
377	5466600	377	11632192	377	7465279
378	5436000	378	11574128	378	7451376
379	5425200	379	11572060	379	7440688
380	5424300	380	11554771	380	7425766
381	5416200	381	11518722	381	7384887
382	5408100	382	11456174	382	7375084
383	5400900	383	11445404	383	7330234
384	5392800	384	11425550	384	7317185
385	5390100	385	11423079	385	7292935
386	5359500	386	11406164	386	7255618
387	5320800	387	11383690	387	7254358
388	5319900	388	11368802	388	7235509
389	5281200	389	11362486	389	7222497
390	5280300	390	11348261	390	7220649
391	5267700	391	11331368	391	7209636
392	5247900	392	11226700	392	7207231
393	5245200	393	11210983	393	7199943
394	5238900	394	11204326	394	7197552
395	5194800	395	11175215	395	7180547
396	5180400	396	11109209	396	7123036
397	5179500	397	11077219	397	7098319
398	5175000	398	11031006	398	7090945
399	5156100	399	11026243	399	7055912
400	5152500	400	11005600	400	7043778
401	5138100	401	10997904	401	7042846
402	5124600	402	10959898	402	7027818
403	5120100	403	10955185	403	7014185
404	5069700	404	10887741	404	7010526
405	5051700	405	10872046	405	7002179
406	5045400	406	10871225	406	7001775
407	5022000	407	10867746	407	6989757
408	4974300	408	10812643	408	6978478
409	4947300	409	10795993	409	6964347
410	4946400	410	10793344	410	6921850
411	4907700	411	10784332	411	6909494
412	4907700	412	10767998	412	6828496

413	4905900	413	10766014	413	6828192
414	4885200	414	10727461	414	6826564
415	4878000	415	10692322	415	6807297
416	4862700	416	10677498	416	6800803
417	4862700	417	10627260	417	6773658
418	4833000	418	10620891	418	6773503
419	4830300	419	10607482	419	6771675
420	4829400	420	10607225	420	6752936
421	4813200	421	10588624	421	6740710
422	4800600	422	10542875	422	6718838
423	4799700	423	10540165	423	6703191
424	4790700	424	10457240	424	6680977
425	4781700	425	10389027	425	6673365
426	4768200	426	10387879	426	6672115
427	4734900	427	10374914	427	6623086
428	4731300	428	10339131	428	6618265
429	4727700	429	10307572	429	6614101
430	4716000	430	10278653	430	6582939
431	4707000	431	10248166	431	6577289
432	4682700	432	10159429	432	6553763
433	4668300	433	10138499	433	6553375
434	4666500	434	10083984	434	6546253
435	4657500	435	10053936	435	6545943
436	4643100	436	10031119	436	6544895
437	4642200	437	10030360	437	6535406
438	4641300	438	10025610	438	6529674
439	4583700	439	10004136	439	6487966
440	4581000	440	9927896	440	6486747
441	4580100	441	9894487	441	6475256
442	4555800	442	9880082	442	6468487
443	4553100	443	9872305	443	6458821
444	4547700	444	9859088	444	6454884
445	4484700	445	9817844	445	6438094
446	4479300	446	9732941	446	6437616
447	4475700	447	9722981	447	6419122
448	4473000	448	9698035	448	6385196
449	4471200	449	9610643	449	6381760
450	4464900	450	9590653	450	6369963
451	4449600	451	9581740	451	6368063
452	4446900	452	9578724	452	6354585
453	4443300	453	9539087	453	6316425
454	4439700	454	9532187	454	6315164
455	4432500	455	9510518	455	6312926
456	4428000	456	9496382	456	6302755
457	4414500	457	9439160	457	6282874
458	4412700	458	9398316	458	6277167
459	4389300	459	9397103	459	6276819
460	4384800	460	9382642	460	6268950
461	4375800	461	9350425	461	6262063
462	4363200	462	9333794	462	6238574
463	4362300	463	9247009	463	6227532
464	4362300	464	9217206	464	6181754
465	4360500	465	9215372	465	6174311
466	4359600	466	9185526	466	6154085
467	4332600	467	9182975	467	6139232
468	4329000	468	9179084	468	6136416
469	4323600	469	9170248	469	6094966
470	4311900	470	9163727	470	6093591
471	4303800	471	9134851	471	6068448
472	4294800	472	9129960	472	6062006
473	4293900	473	9121398	473	6057547
474	4284000	474	9119039	474	6039917
475	4283100	475	9114430	475	6029919
476	4281300	476	9088671	476	6028745
477	4280400	477	9063102	477	6027612
478	4267800	478	9045106	478	6025533
479	4261500	479	9038711	479	5999202
480	4253400	480	9020585	480	5995620
481	4243500	481	8994862	481	5990082
482	4234500	482	8976914	482	5988048
483	4229100	483	8961558	483	5984265
484	4226400	484	8960520	484	5981997
485	4221000	485	8948784	485	5981975
486	4221000	486	8928033	486	5980921
487	4204800	487	8919367	487	5974046
488	4169700	488	8916341	488	5971190
489	4155300	489	8901000	489	5967521
490	4122000	490	8880682	490	5945482
491	4113900	491	8874518	491	5916697
492	4102200	492	8861174	492	5916036
493	4095900	493	8851638	493	5865786
494	4094100	494	8814623	494	5864888

495	4066200	495	8807787	495	5855496
496	4065300	496	8780797	496	5845675
497	4063500	497	8779125	497	5845225
498	4054500	498	8771417	498	5840170
499	4036500	499	8771045	499	5838629
500	4031100	500	8747594	500	5828989
501	4028400	501	8746682	501	5817607
502	4025700	502	8737250	502	5803648
503	4017600	503	8705642	503	5778571
504	4011300	504	8669064	504	5774200
505	4005000	505	8629185	505	5773866
		506	8600821	506	5766800
		507	8598983	507	5754347
		508	8569661	508	5752395
		509	8544066	509	5751945
		510	8459664	510	5731050
		511	8447268	511	5727342
		512	8431045	512	5719866
		513	8401608	513	5703917
		514	8393943	514	5693018
		515	8372351	515	5680444
		516	8338828	516	5678729
		517	8335248	517	5667667
		518	8299293	518	5658227
		519	8280368	519	5652682
		520	8274665	520	5650045
		521	8271165	521	5646814
		522	8271017	522	5639156
		523	8269280	523	5638109
		524	8265325	524	5633939
		525	8252804	525	5630736
		526	8211876	526	5628600
		527	8207835	527	5619778
		528	8196549	528	5607240
		529	8174641	529	5595341
		530	8140069	530	5587210
		531	8136667	531	5585814
		532	8119531	532	5583431
		533	8118424	533	5563143
		534	8108668	534	5559985
		535	8099646	535	5520269
		536	8080242	536	5504810
		537	8049384	537	5501139
		538	8038976	538	5491121
		539	8017173	539	5474651
		540	8015329	540	5464196
		541	8009516	541	5464120
		542	7974205	542	5459501
		543	7963445	543	5450234
		544	7920269	544	5420848
		545	7915201	545	5416491
		546	7894540	546	5411337
		547	7893262	547	5409075
		548	7842968	548	5405265
		549	7836814	549	5401631
		550	7814274	550	5391376
		551	7799179	551	5363538
		552	7789779	552	5351687
		553	7739922	553	5344625
		554	7738863	554	5342410
		555	7729888	555	5336563
		556	7704769	556	5322714
		557	7699969	557	5314215
		558	7676840	558	5307550
		559	7645261	559	5304785
		560	7625998	560	5283236
		561	7622774	561	5282677
		562	7620865	562	5279014
		563	7615636	563	5269078
		564	7605295	564	5251398
		565	7593494	565	5213195
		566	7589188	566	5205934
		567	7574265	567	5197977
		568	7573002	568	5195266
		569	7567189	569	5194196
		570	7557484	570	5187474
		571	7542936	571	5183846
		572	7539590	572	5180309
		573	7536592	573	5176895
		574	7531995	574	5159224
		575	7516412	575	5153156
		576	7513557	576	5143837
		577	7511996	577	5124658

					578	7502681			578	5123034				
					579	7502625			579	5119722				
					580	7487205			580	5113224				
					581	7456120			581	5101727				
					582	7445479			582	5100169				
					583	7394358			583	5099744				
					584	7389664			584	5081224				
					585	7360624			585	5066844				
					586	7340446			586	5065661				
					587	7329290			587	5020438				
					588	7327510			588	5014378				
					589	7323381			589	4985701				
					590	7304003			590	4980224				
					591	7275863			591	4964451				
					592	7271521			592	4957065				
					593	7205562			593	4951431				
					594	7199660			594	4924999				
					595	7189222			595	4899828				
					596	7162397			596	4895494				
					597	7145957			597	4893884				
					598	7137329			598	4889936				
					599	7135125			599	4887810				
					600	7131440			600	4880023				
					601	7117920			601	4875423				
					602	7106353			602	4872304				
					603	7093625			603	4865692				
					604	7060179			604	4843796				
					605	7042782			605	4836152				
					606	6988896			606	4833157				
					607	6985122			607	4829347				
					608	6945034			608	4810802				
					609	6942924			609	4790478				
					610	6915755			610	4789237				
					611	6898313			611	4784948				
					612	6893994			612	4768145				
					613	6887027			613	4762957				
					614	6880753			614	4759469				
					615	6873253			615	4755090				
					616	6862865			616	4754767				
					617	6846183			617	4751359				
					618	6840563			618	4744614				
					619	6823237			619	4739933				
					620	6809511			620	4730512				
					621	6805236			621	4722871				
					622	6802461			622	4709557				
					623	6788876			623	4708714				
					624	6776181			624	4672183				
					625	6761865			625	4665258				
					626	6746691			626	4662951				
					627	6738583			627	4662702				
					628	6720951			628	4659395				
					629	6720653			629	4652212				
					630	6710435			630	4649481				
					631	6709898			631	4648608				
					632	6708013			632	4635307				
					633	6705329			633	4630122				
					634	6699769			634	4599426				
					635	6687402			635	4595734				
					636	6657926			636	4593159				
					637	6634936			637	4574157				
					638	6629595			638	4562160				
					639	6624549			639	4561879				
					640	6620808			640	4549320				
					641	6610331			641	4545873				
					642	6580573			642	4545590				
					643	6580486			643	4544007				
					644	6576910			644	4541354				
					645	6548961			645	4540972				
					646	6543265			646	4539398				
					647	6542110			647	4536972				
					648	6531189			648	4532652				
					649	6529283			649	4531934				
					650	6515415			650	4528386				
					651	6500129			651	4520460				
					652	6498963			652	4511218				
					653	6492329			653	4509201				
					654	6484213			654	4501150				
					655	6478076			655	4495468				
					656	6452516			656	4489787				
					657	6436849			657	4488431				
					658	6436467			658	4461261				
					659	6403341			659	4461190				
					660	6376483			660	4447285				

					661	6375433			661	4443195				
					662	6358754			662	4438111				
					663	6357131			663	4437799				
					664	6317657			664	4426675				
					665	6317625			665	4424523				
					666	6309037			666	4415951				
					667	6301769			667	4396816				
					668	6296883			668	4389155				
					669	6278040			669	4384631				
					670	6264387			670	4367020				
					671	6255364			671	4364685				
					672	6223151			672	4341184				
					673	6219251			673	4336333				
					674	6217738			674	4315623				
					675	6211232			675	4311248				
					676	6205431			676	4300311				
					677	6204026			677	4296518				
					678	6197842			678	4285140				
					679	6179560			679	4282653				
					680	6161309			680	4280673				
					681	6159629			681	4274980				
					682	6140870			682	4272086				
					683	6129733			683	4271026				
					684	6096533			684	4261642				
					685	6090056			685	4258234				
					686	6082953			686	4255779				
					687	6078588			687	4249222				
					688	6064939			688	4249210				
					689	6063123			689	4246070				
					690	6044730			690	4235777				
					691	6044670			691	4235381				
					692	6041312			692	4231223				
					693	6017345			693	4221558				
					694	5990498			694	4218067				
					695	5981933			695	4215787				
					696	5974621			696	4211303				
					697	5974116			697	4195018				
					698	5973010			698	4190760				
					699	5957151			699	4189247				
					700	5956118			700	4189211				
					701	5952472			701	4189114				
					702	5913621			702	4189071				
					703	5878508			703	4180225				
					704	5852939			704	4177543				
					705	5850587			705	4169591				
					706	5844538			706	4168928				
					707	5833286			707	4164073				
					708	5831538			708	4154719				
					709	5814002			709	4151392				
					710	5805116			710	4146480				
					711	5798204			711	4144890				
					712	5782311			712	4144400				
					713	5770312			713	4136996				
					714	5719241			714	4126057				
					715	5712427			715	4124337				
					716	5703420			716	4118653				
					717	5701940			717	4116008				
					718	5688741			718	4111418				
					719	5687300			719	4110164				
					720	5680464			720	4107438				
					721	5678702			721	4107133				
					722	5675667			722	4097369				
					723	5655324			723	4093783				
					724	5648553			724	4091260				
					725	5645103			725	4089102				
					726	5642992			726	4081898				
					727	5635791			727	4081307				
					728	5631619			728	4080335				
					729	5621806			729	4078353				
					730	5604979			730	4073951				
					731	5586422			731	4065106				
					732	5586159			732	4059022				
					733	5571191			733	4052711				
					734	5569379			734	4049578				
					735	5569163			735	4045848				
					736	5542641			736	4045158				
					737	5540115			737	4042449				
					738	5527283			738	4039770				
					739	5524029			739	4037077				
					740	5508496			740	4026854				
					741	5507897			741	4024446				
					742	5504308			742	4021440				

					743	5496438			743	4015824				
					744	5486794			744	4011606				
					745	5462240			745	4001294				
					746	5454711								
					747	5437501								
					748	5436434								
					749	5424443								
					750	5420580								
					751	5412221								
					752	5400398								
					753	5389969								
					754	5387934								
					755	5370738								
					756	5367283								
					757	5360796								
					758	5357734								
					759	5354404								
					760	5331858								
					761	5320608								
					762	5312361								
					763	5283152								
					764	5269563								
					765	5254755								
					766	5233165								
					767	5201309								
					768	5200855								
					769	5198573								
					770	5192112								
					771	5184462								
					772	5182455								
					773	5178569								
					774	5163570								
					775	5144200								
					776	5135094								
					777	5133059								
					778	5132623								
					779	5130978								
					780	5130376								
					781	5125299								
					782	5124752								
					783	5101632								
					784	5093228								
					785	5077507								
					786	5066942								
					787	5064878								
					788	5060163								
					789	5051420								
					790	5045229								
					791	5039717								
					792	5038744								
					793	5024177								
					794	5003955								
					795	4983674								
					796	4983616								
					797	4977284								
					798	4969687								
					799	4960832								
					800	4958375								
					801	4952320								
					802	4951342								
					803	4936269								
					804	4929404								
					805	4912222								
					806	4908897								
					807	4879178								
					808	4870227								
					809	4860221								
					810	4850275								
					811	4836305								
					812	4827969								
					813	4827911								
					814	4816746								
					815	4812866								
					816	4812366								
					817	4810655								
					818	4800604								
					819	4800293								
					820	4794507								
					821	4791083								
					822	4786862								
					823	4779842								
					824	4777770								
					825	4773890								

					826	4769992								
					827	4768613								
					828	4766050								
					829	4763884								
					830	4760982								
					831	4756323								
					832	4756011								
					833	4751561								
					834	4748381								
					835	4747899								
					836	4740177								
					837	4731560								
					838	4715118								
					839	4714433								
					840	4707773								
					841	4706377								
					842	4693443								
					843	4676253								
					844	4667158								
					845	4655948								
					846	4653551								
					847	4637195								
					848	4632058								
					849	4625651								
					850	4625350								
					851	4619570								
					852	4615032								
					853	4609031								
					854	4604042								
					855	4603870								
					856	4602971								
					857	4592625								
					858	4586319								
					859	4585659								
					860	4576907								
					861	4575528								
					862	4568267								
					863	4567990								
					864	4563446								
					865	4550516								
					866	4521750								
					867	4521678								
					868	4512280								
					869	4495402								
					870	4494179								
					871	4483658								
					872	4480149								
					873	4469423								
					874	4468589								
					875	4457934								
					876	4450611								
					877	4447613								
					878	4446518								
					879	4441947								
					880	4441704								
					881	4437698								
					882	4423975								
					883	4421239								
					884	4418596								
					885	4410724								
					886	4407881								
					887	4405563								
					888	4404443								
					889	4396815								
					890	4389956								
					891	4384967								
					892	4381911								
					893	4377577								
					894	4376843								
					895	4372448								
					896	4371358								
					897	4361302								
					898	4351292								
					899	4350308								
					900	4325171								
					901	4313679								
					902	4313217								
					903	4310312								
					904	4304672								
					905	4292466								
					906	4290572								
					907	4288394								
					908	4284324								

					909	4282792								
					910	4280537								
					911	4276090								
					912	4265936								
					913	4261028								
					914	4260884								
					915	4256451								
					916	4255265								
					917	4247280								
					918	4244370								
					919	4235765								
					920	4235018								
					921	4226598								
					922	4223854								
					923	4210181								
					924	4203166								
					925	4199680								
					926	4195129								
					927	4192574								
					928	4188131								
					929	4187168								
					930	4163647								
					931	4160612								
					932	4158000								
					933	4143192								
					934	4131832								
					935	4124924								
					936	4091900								
					937	4090116								
					938	4087067								
					939	4077816								
					940	4075174								
					941	4068762								
					942	4062578								
					943	4062106								
					944	4057712								
					945	4040104								
					946	4037201								
					947	4033959								
					948	4026811								
					949	4024465								
					950	4019194								
					951	4018215								
					952	4011787								
					953	4010547								
					954	4009029								
					955	4002701								
					956	4001318								
					957	3992767								
					958	3992273								
					959	3972944								
					960	3969889								
					961	3962187								
					962	3958800								
					963	3954418								
					964	3952559								
					965	3951460								
					966	3950320								
					967	3949490								
					968	3945612								
					969	3942690								
					970	3941596								
					971	3941124								
					972	3940747								
					973	3934625								
					974	3933503								
					975	3930270								
					976	3926426								
					977	3925734								
					978	3923487								
					979	3922514								
					980	3919222								
					981	3918804								
					982	3917209								
					983	3916463								
					984	3912270								
					985	3912138								
					986	3910947								
					987	3909399								
					988	3902567								
					989	3902021								
					990	3898761								
					991	3897059								

					992	3893864								
					993	3887121								
					994	3879185								
					995	3870763								
					996	3869976								
					997	3863912								
					998	3860009								
					999	3856392								
					1000	3847687								
					1001	3844189								
					1002	3843354								
					1003	3842105								
					1004	3839528								
					1005	3839407								
					1006	3838717								
					1007	3836459								
					1008	3835822								
					1009	3835724								
					1010	3829896								
					1011	3828034								
					1012	3822169								
					1013	3821360								
					1014	3816595								
					1015	3816577								
					1016	3808367								
					1017	3806890								
					1018	3802728								
					1019	3790175								
					1020	3789129								
					1021	3786628								
					1022	3783772								
					1023	3775442								
					1024	3770851								
					1025	3764892								
					1026	3762684								
					1027	3756767								
					1028	3755329								
					1029	3750186								
					1030	3749566								
					1031	3739976								
					1032	3736089								
					1033	3730135								
					1034	3729958								
					1035	3725947								
					1036	3718166								
					1037	3711644								
					1038	3691510								
					1039	3681621								
					1040	3675758								
					1041	3668197								
					1042	3660967								
					1043	3646170								
					1044	3645295								
					1045	3642105								
					1046	3636846								
					1047	3632151								
					1048	3631485								
					1049	3626300								
					1050	3624654								
					1051	3623625								
					1052	3618926								
					1053	3614444								
					1054	3610320								
					1055	3604029								
					1056	3599911								
					1057	3591707								
					1058	3590619								
					1059	3587771								
					1060	3585403								
					1061	3579363								
					1062	3578356								
					1063	3567342								
					1064	3553970								
					1065	3548873								
					1066	3546971								
					1067	3543426								
					1068	3543355								
					1069	3542014								
					1070	3537852								
					1071	3534640								
					1072	3530267								
					1073	3526341								
					1074	3523939								

					1075	3518796								
					1076	3508867								
					1077	3501361								
					1078	3500103								

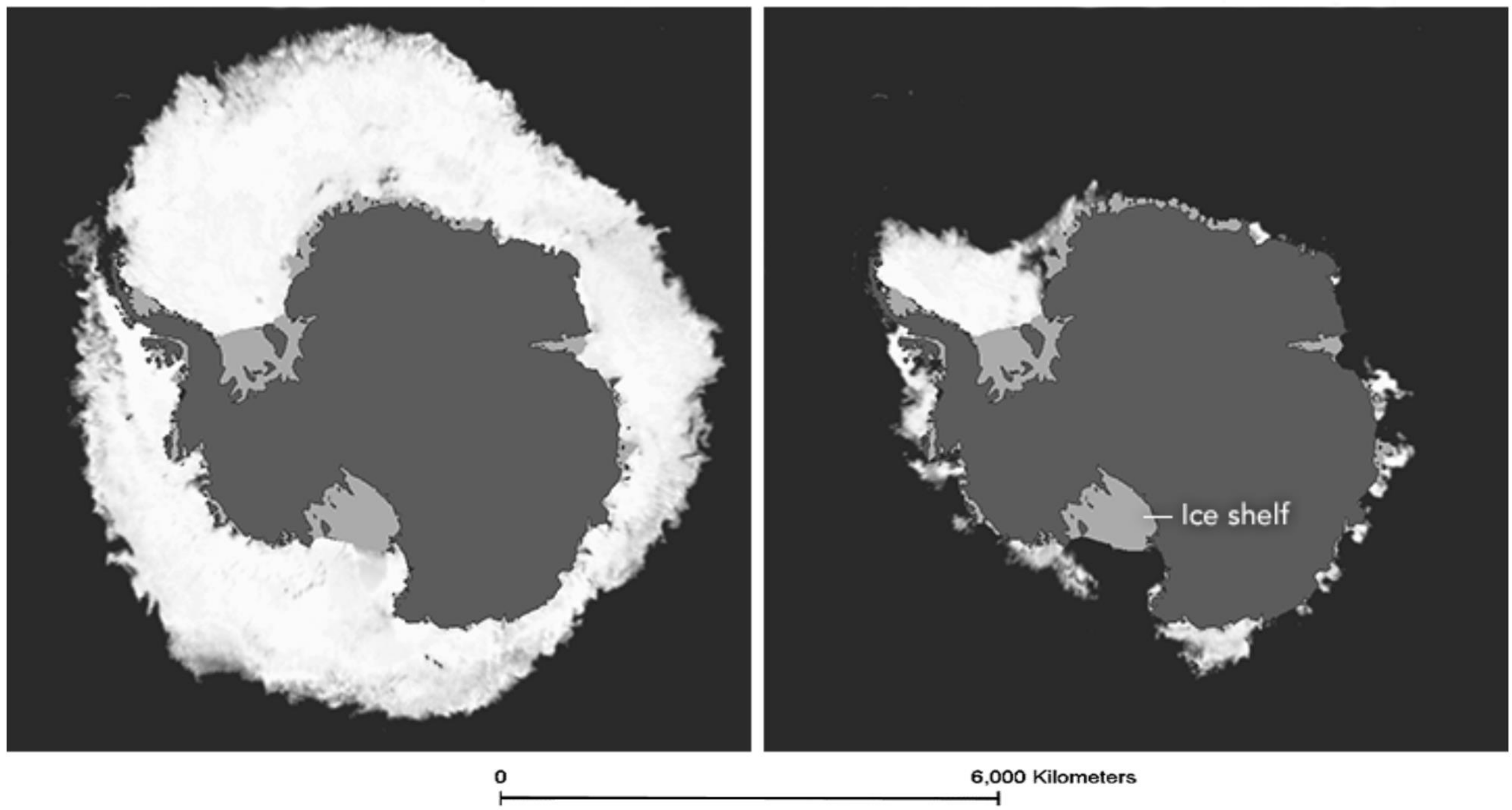

Figure 1. Satellite image showing the extent of Antarctic sea ice cover on October 6, 2016 (left) and February 19, 2016 (right). Water is black, sea ice is white, land is dark grey, and ice shelfves are light grey. Figures are from the USGS Earth Observatory https://earthobservatory.nasa.gov/features/SeaIce/page4.php

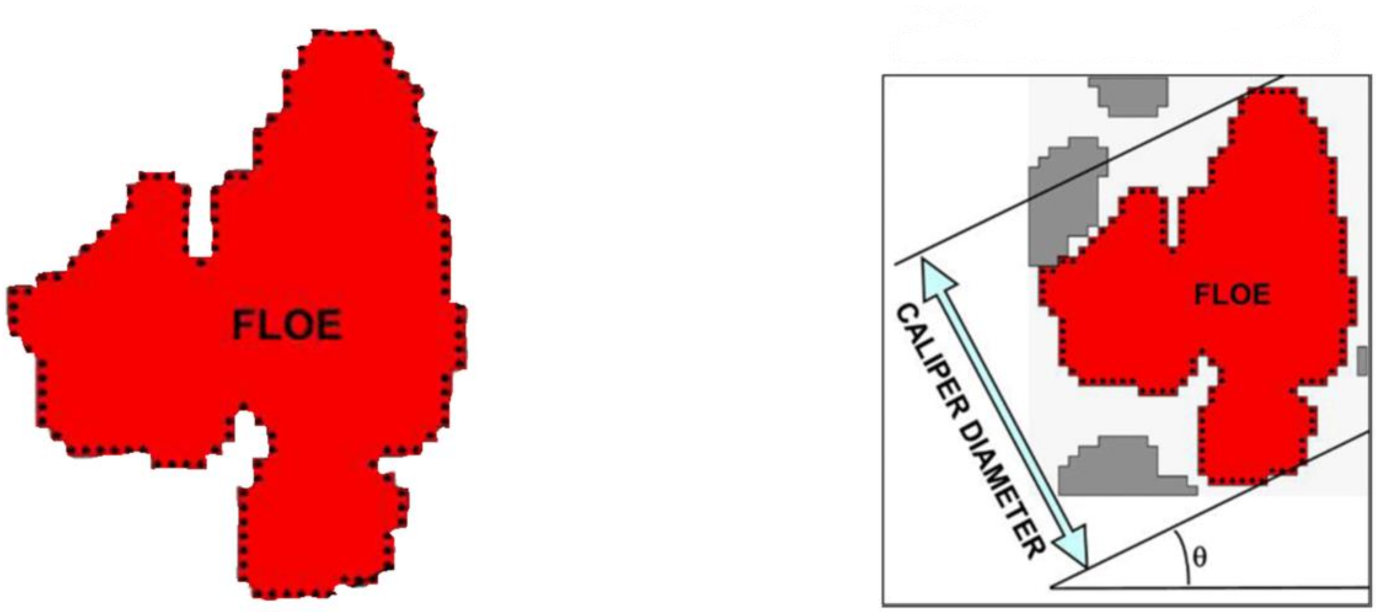

Figure 2. Two methods were used to approximate the floe area. Method on the left counts pixels on digitized images, which was used in this study. On the rightt is the mean caliper-diameter method which approximates the area by measuring the distance between parallel calipers tangent to opposite sides of the floe and calculating the mean distance over all orientations θ of the calipers. Note, that in the mean caliper-diameter method, the area of the floe is not calculated from the mean caliper-diameter. This figure is modified from Figure 2 in Stern and others, 2018

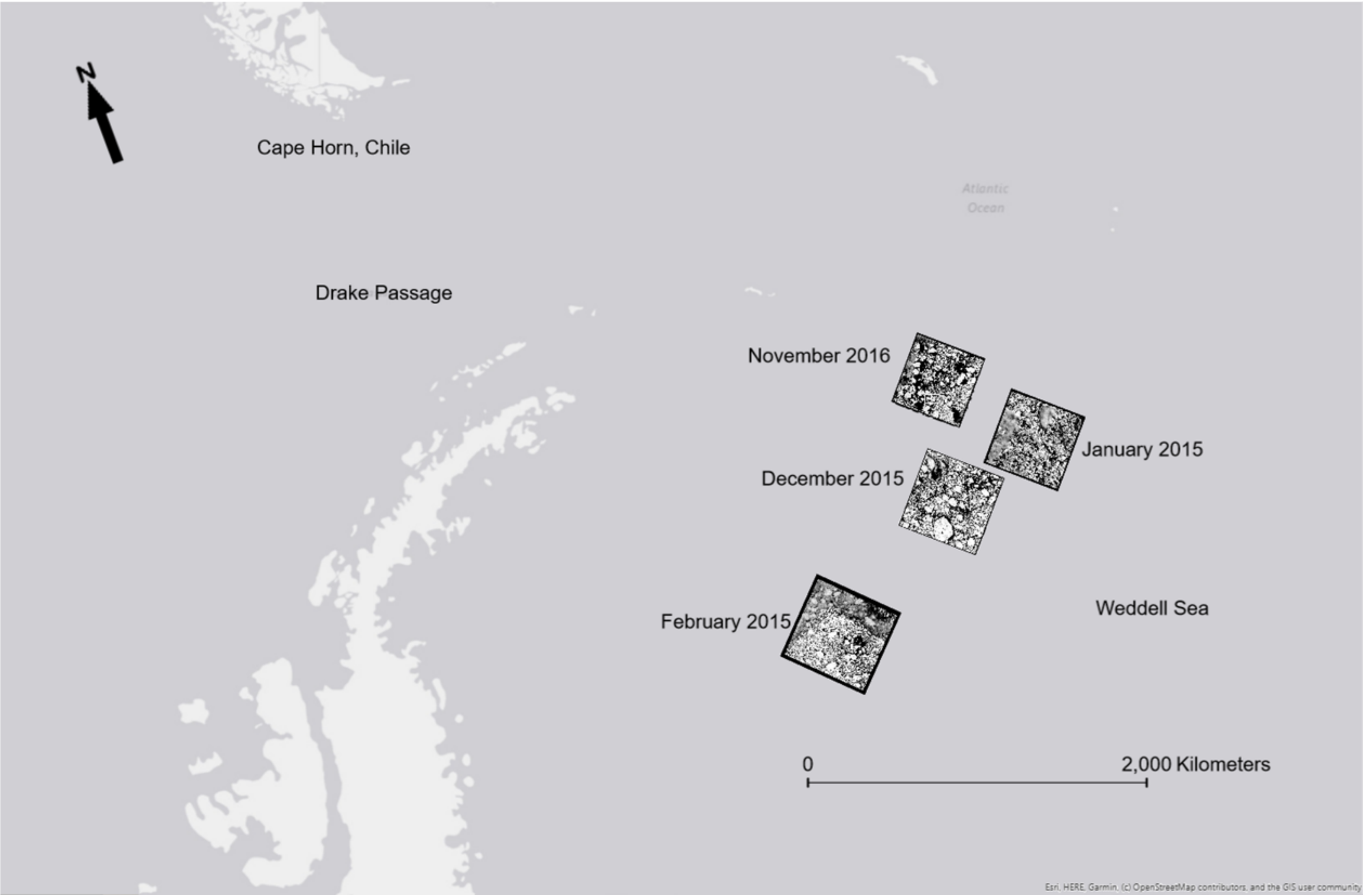

Figure 3. Image showing location of the ice floe images in the Weddell Sea used in this study. Figure was created in Arc PRO (ESRI) the ice floe images are from (November 2016, Image Number (LC08_L1GT_202104_20161105), December 2015 Image Number (LC08_L1GT_200106_20151207), January 2015 Image Number (LC08_L1GT_198105_20150107), and February 2015 Image Number (LC08_L1GT_202108_20150220) USGS Earth Explorer.

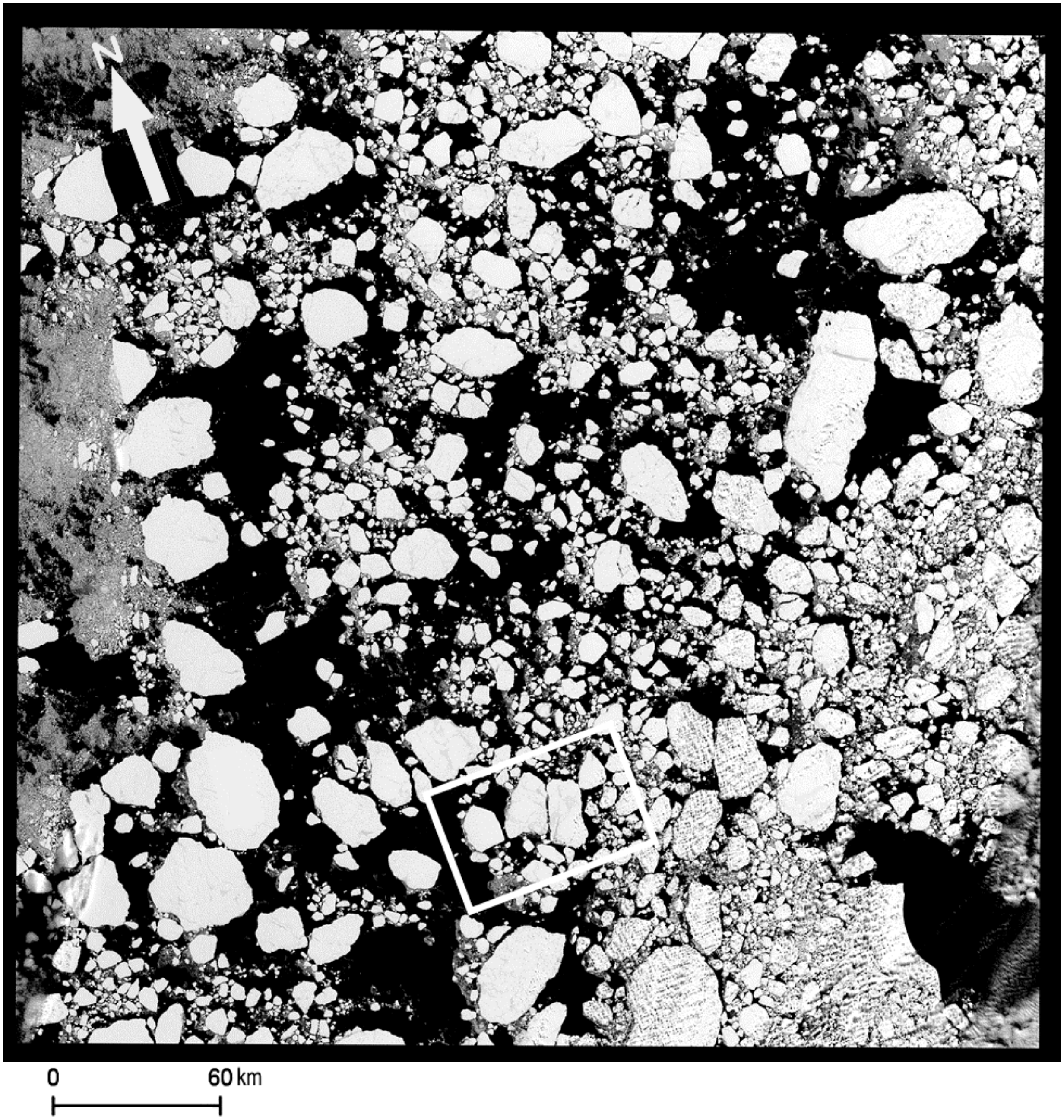

Figure 4a. (05 November 2016) Satellite image of ice floes in the Weddell Sea. The white rectangular inset marks the location of Figure 4b. Image Number LC08_L1GT_202104_20161105 USGS Earth Explorer https://earthexplorer.usgs.gov/

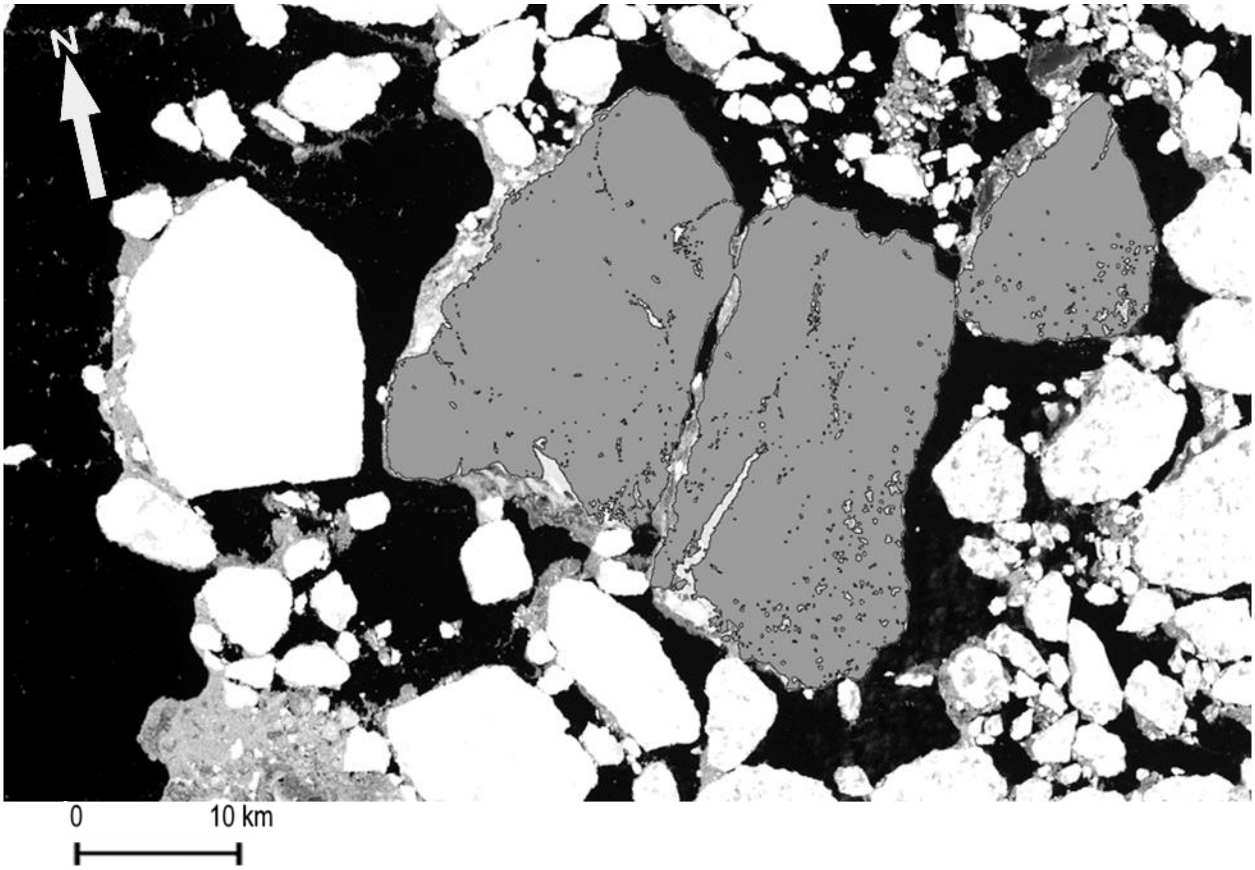

Figure 4b. (05 November 2016) Image of ice floes in the Weddell Sea showing the larger floes (grey) being cushioned by smaller ice floes; larger floes (grey). Cushioning of the larger flows reduces the probability of size reduction by fracturing. Note that the cushioning is present for almost all sizes which may mean that once the floe size distribution is established at the time of the initial breakup, further size reduction is primarily by grinding and melting of the floe edges and not by fracturing across the floes. (ESRI). The location of this figure is shown by the rectangle in Figure 4a. Image Number LC08_L1GT_202104_20161105 USGS Earth Explorer https://earthexplorer.usgs.gov/

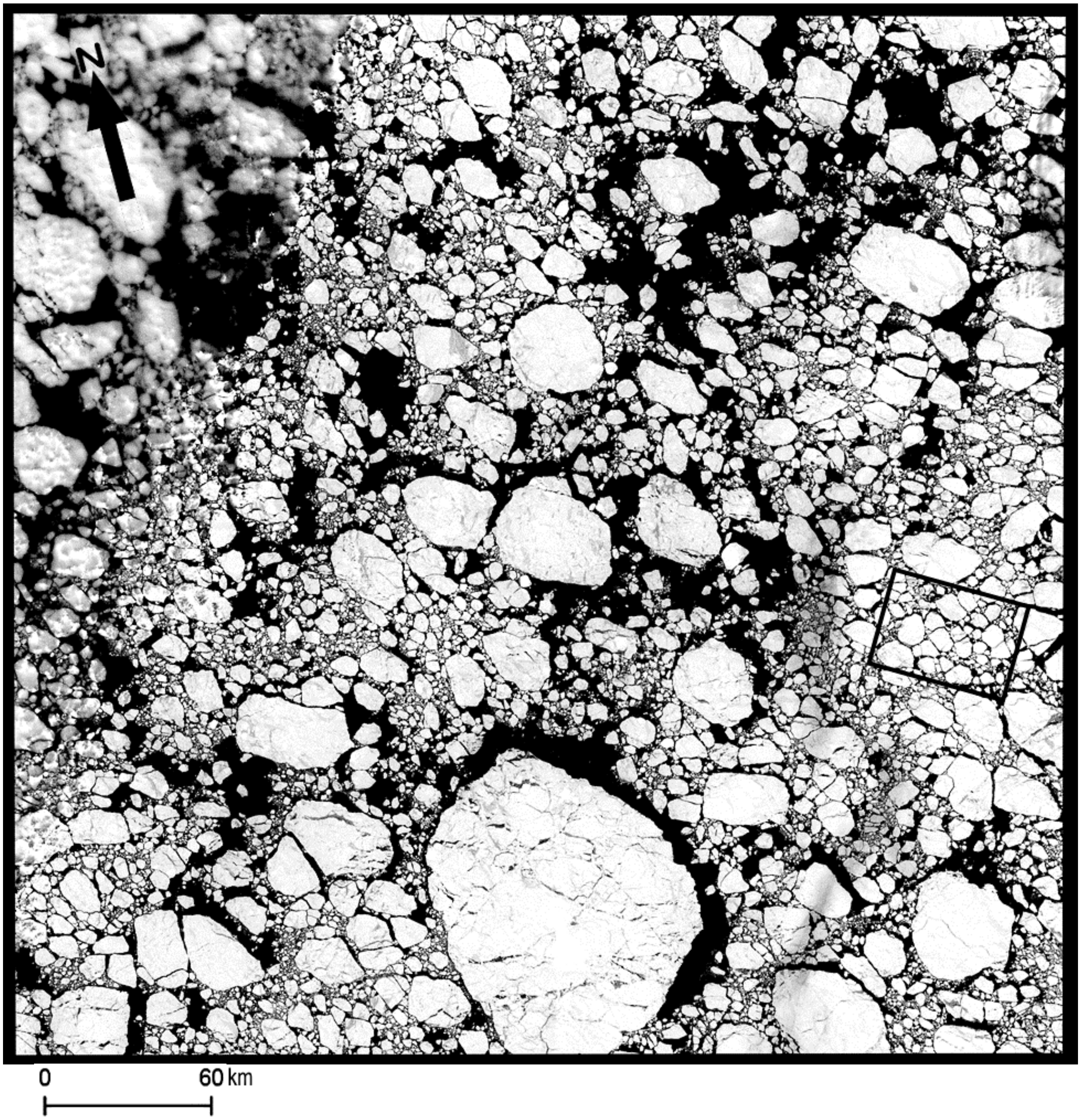

Figure 5a. (07 December 2015) Satellite image of ice floes in the Weddell Sea. The black rectangular inset marks the location of Figure 4b. Image number LC08_L1GT_200106_20151207 USGS Earth Explorer https://earthexplorer.usgs.gov/

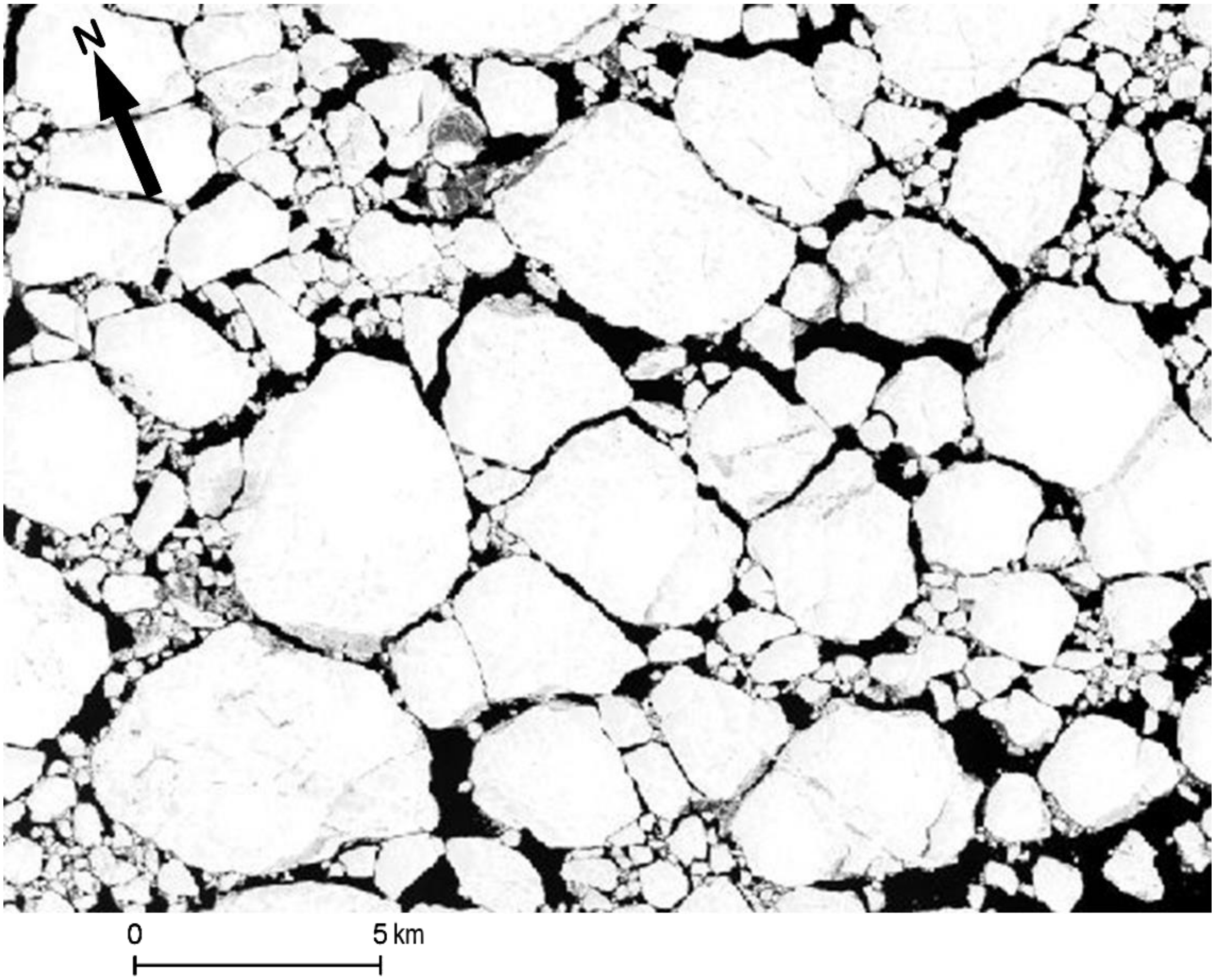

Figure 5b. (07 December 2015) Close up of satellite image soon after the initial breakup of sea ice by the process of fracture. The irregular lines visible within each floe are fused boundaries between old floe that compose the ice pack. See Figure 4a for location. Image Number LC08_L1GT_200106_20151207 USGS Earth Explorer https://earthexplorer.usgs.gov/

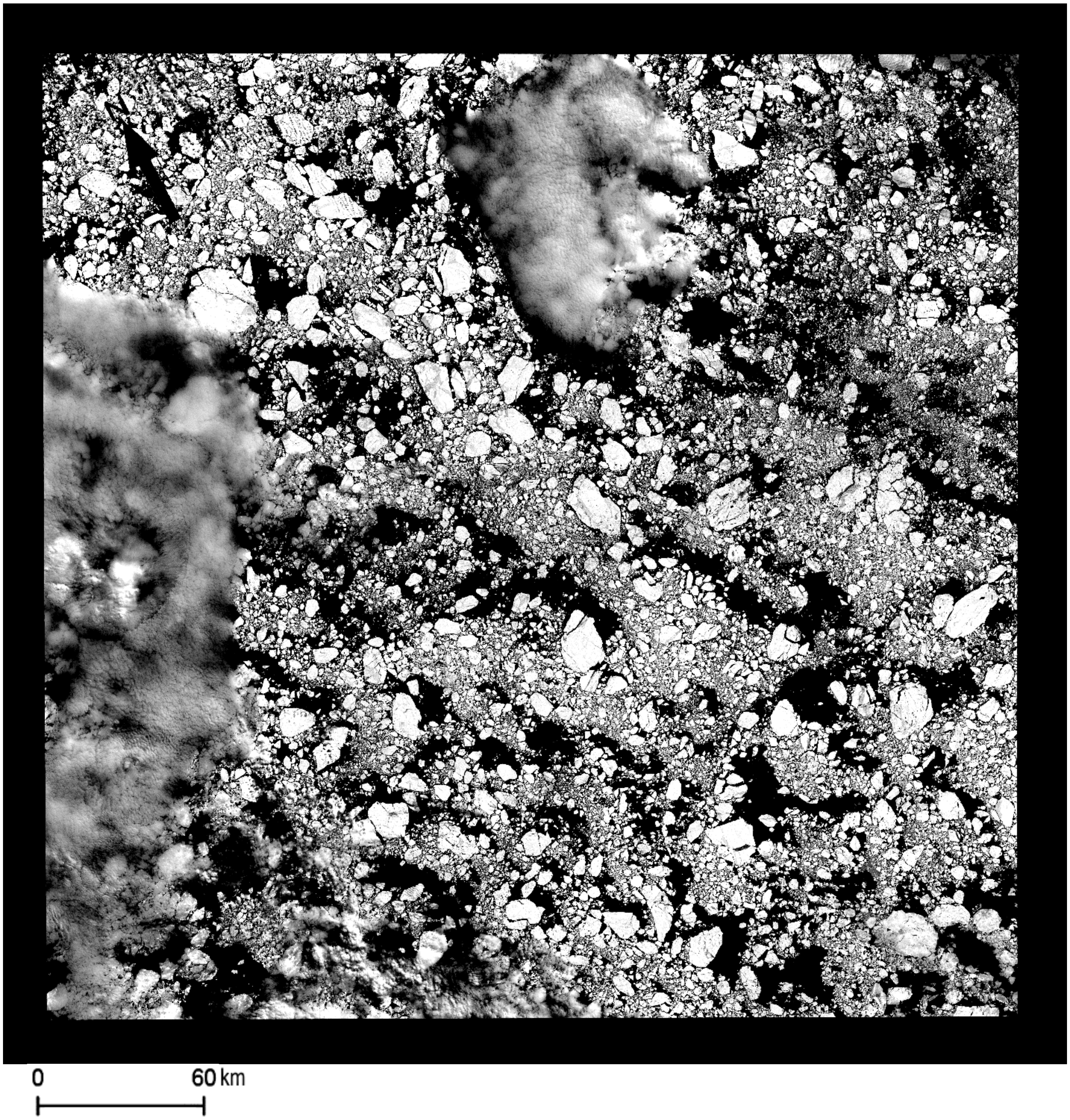

Figure 6. (07 January 2015) Satellite image of ice floes in the Weddell Sea. Image number LC08_L1GT_198105_20150107 USGS Earth Explorer https://earthexplorer.usgs.gov/. The top center and left regions of the image appear out of focus as a result of cloud cover.

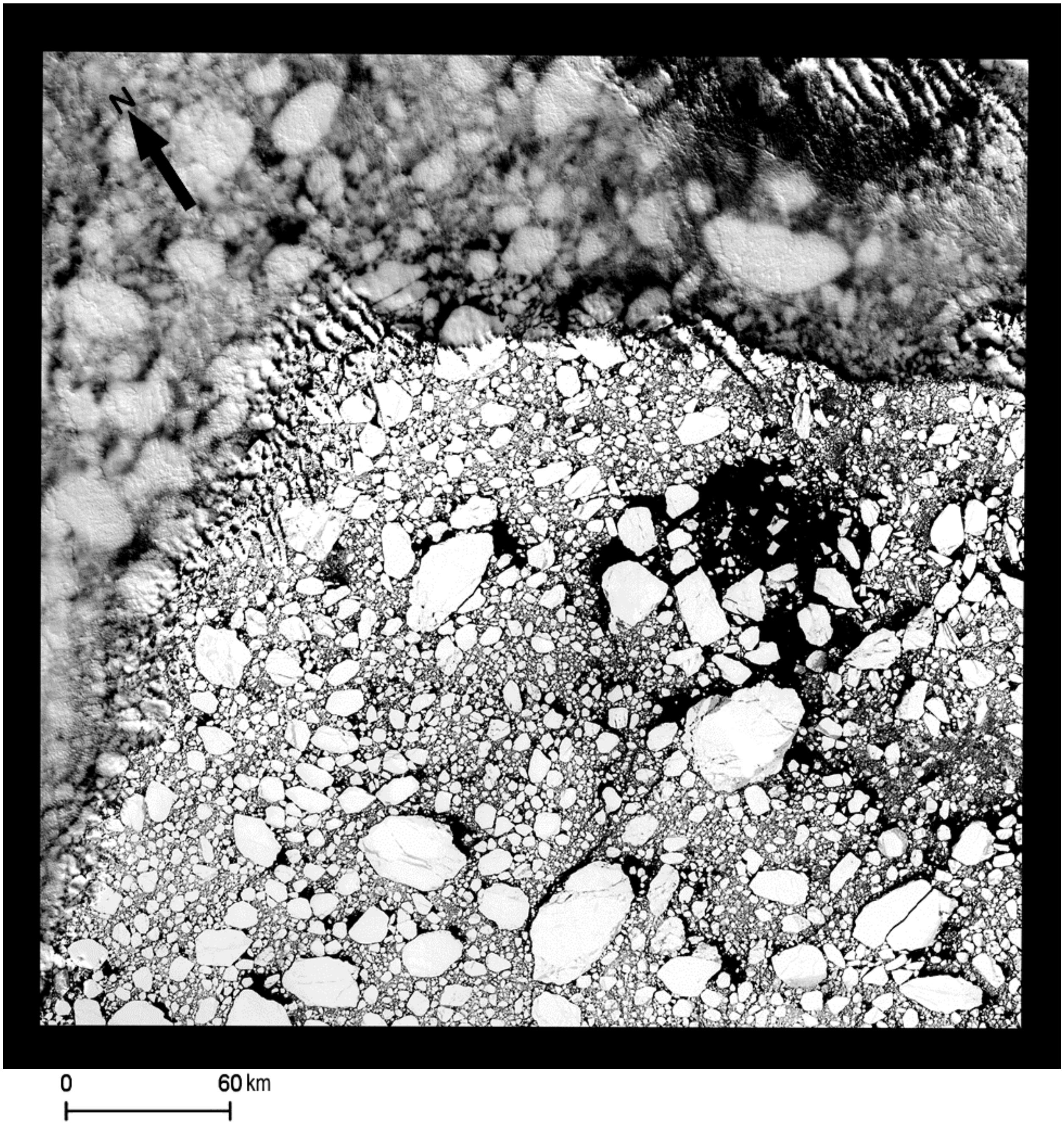

Figure 7. 20 February 2015 Satellite Image of ice floes in the Weddell Sea. Number LC08_L1GT_202108_20150220 USGS Earth Explorer https://earthexplorer.usgs.gov/. The top and left regions of the image appear out of focus as a result of cloud cover.

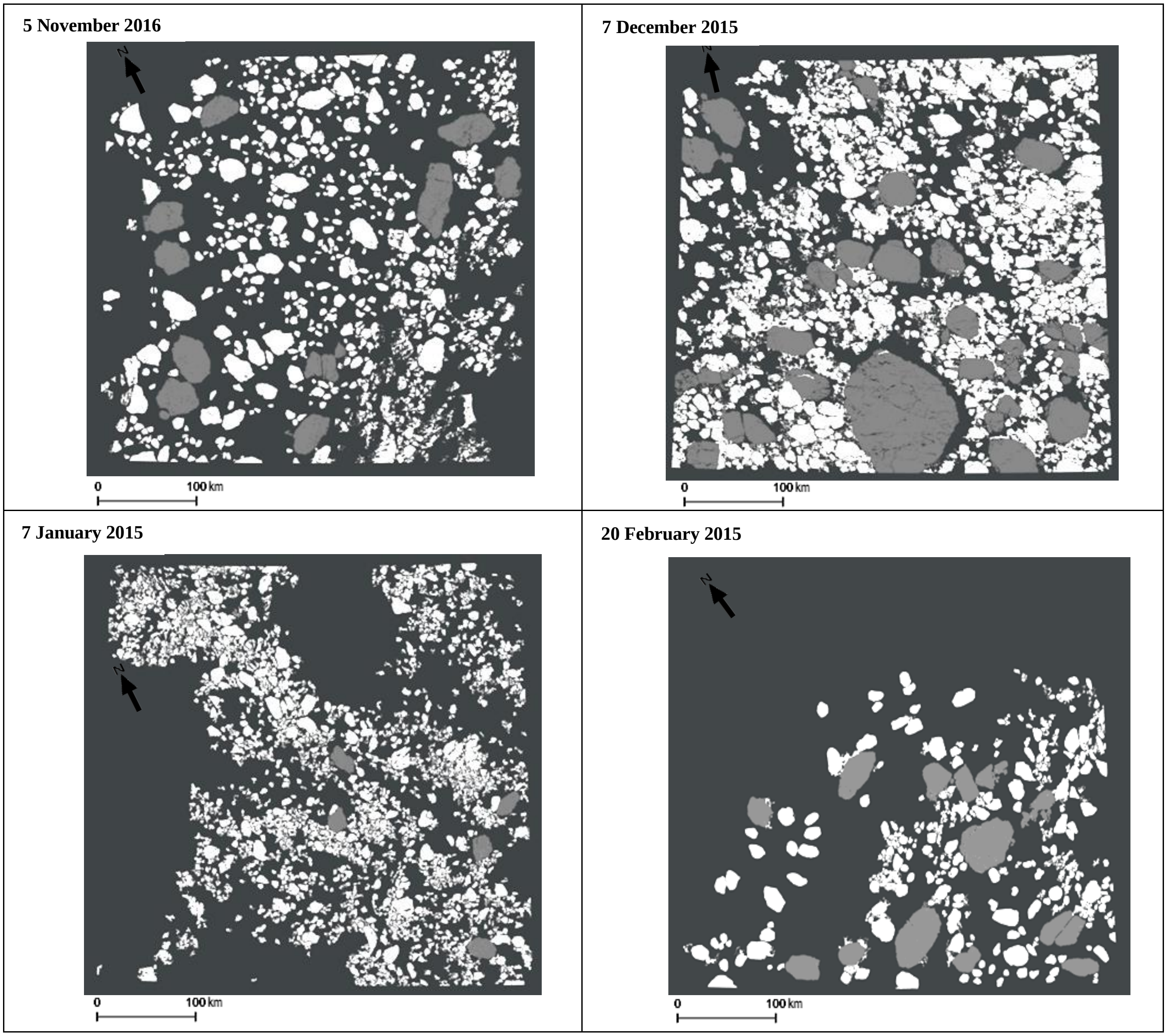

Figure 8. Shape files of satellite images of four floe packs at different stages of fragmentation and floe pack density, during the months of November 2016 Image Number (LC08_L1GT_202104_20161105), December 2015 Image Number (LC08_L1GT_200106_20151207), January 2015 Image Number (LC08_L1GT_198105_20150107), and February 2015 Image Number (LC08_L1GT_202108_20150220) in the study area within the Weddell Sea. Floes partially cut off by image boundaries were not included in the analysis. Floes with areas greater than the inflection point are gray, floes with areas smaller than the inflection point are white, and water is black. Note slush/finely crushed ice and clouds have been removed and were not included in this analysis. USGS Earth Explorer https://earthexplorer.usgs.gov/

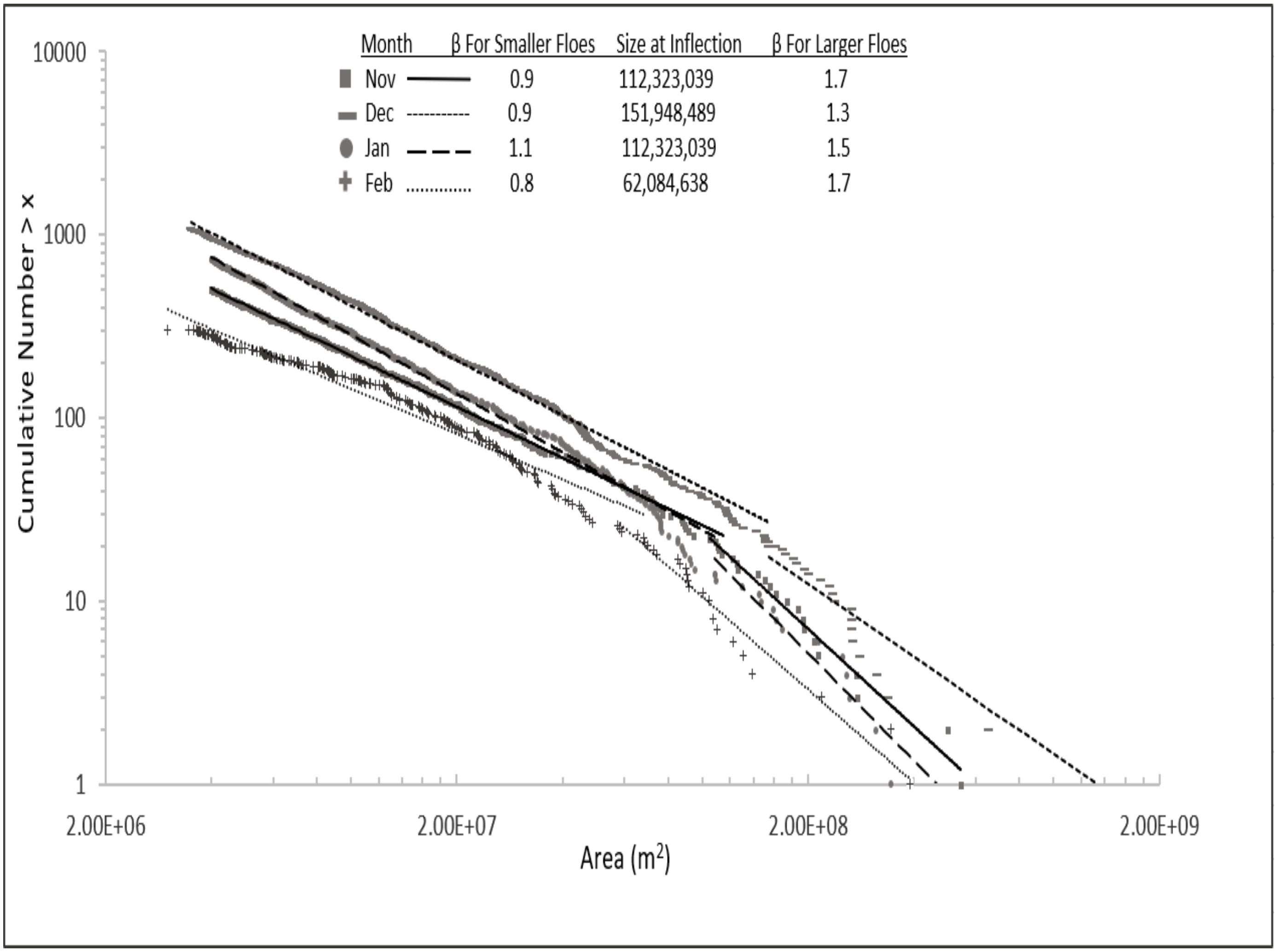

Figure 9. Ice Floe Areas Vs. Cumulative Number for the Weddell Sea Antarctic Ice Floes from USGS Satellite Images. Four images ranging over the arctic summer from early November to mid-February for 2015 and 2016. The data from each image is fit by two power functions. The scaling exponents for the larger floes (1.3-1.7) are consistently greater than those for the smaller floes (0.8-1.1). The power scaling exponents are listed in Table 1.

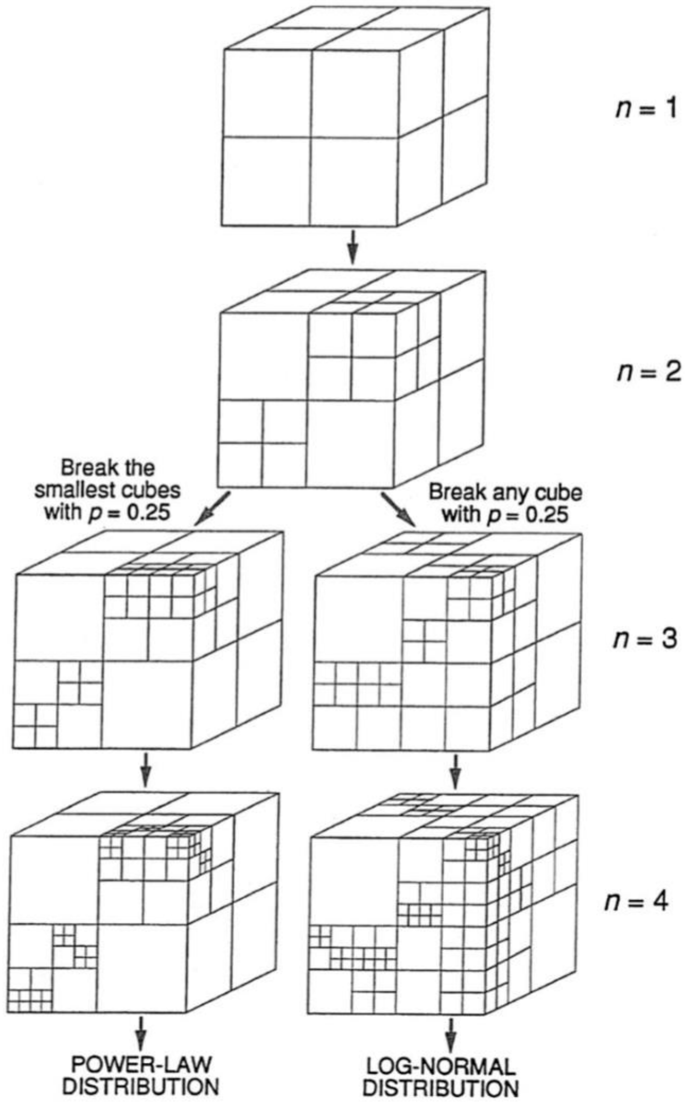

Figure 10. Four iterations (n) in the fragmentation of a unit cube. On left, the constant probability of fragmentation p = 0.25 is for only the smallest cubes to be broken at each iteration resulting in a power fragment size distribution. The constant probability of fragmentation p = 0.25 is for any cube to be broken at each iteration resulting in a lognormal fragment size distribution.

Table 1: Summary of power scaling exponents for fragmentation distribution of ice floes in the Weddell Sea (present study), previous floe size studies in the Antarctic and Artic Oceans. The power scaling exponents are those reported in the referenced studies. The power scaling exponents have been converted from caliper-diameter in parentheses ( ) and non-cumulative values in square brackets [ ] to cumulative area values as described in the text.

Table 1 Summary of present and previous Antarctic and Artic Ice Floe Distributions

				Area					Caliper Diameter							
Location	Time Range	Data Source	Cum.	β < Inflection (m^2)	β > Inflection (m^2)	β No Inflection (m^2)	Range of Floe Areas (m^2)	Area at Inflection (m^2)	β < Inflection (m)	β > Inflection (m)	β No Inflection (m)	Range of floe diameters (m)	Diameter at Inflection (m)	Percent large floes/total floe area	Number of Images	References
ANTARCTIC																ANTARCTIC
Weddell Sea	Nov. 11, 2016	Satellite	Cum.	-0.9	-1.7	-	4,005,000 to 550,000,000	112,323,039	-	-	-	-	-	38	1	Coffey, Barton, and Tebbens (2020)
Weddell Sea	Dec. 7, 2015	Satellite	Cum.	-0.9	-1.6	-	3,500,000 to 345,000,000	151,948,489	-	-	-	-	-	22	1	Coffey, Barton, and Tebbens (2020)
Weddell Sea	Jan. 7, 2015	Satellite	Cum.	-0.8	-1.5	-	4,001,000 to 345,000,000	112,323,039	-	-	-	-	-	21	1	Coffey, Barton, and Tebbens (2020)
Weddell Sea	Feb. 20, 2015	Satellite	Cum.	-0.8	-1.5	-	3,000,000 to 390,000,000	62,084,638	-	-	-	-	-	44	1	Coffey, Barton, and Tebbens (2020)
Weddell Sea, Montagu Island	Spring 2003	Aerial, Satellite	Non-Cum.	-	-	-	-	-	-	-	–2.0 (-3.0) [-4.0]	2 to 100	-	-	1	Gherardi and Lagomarsino (2015)
Weddell Sea	Feb. 1990	Aerial	Cum.	-	-	-0.68	1 to 350	-	-	-	-	-	-	-	1	Lensu (1990)
Prydz Bay, East Antarctic	Dec. 2004 - Feb. 2005	Aerial, Satellite	Cum.	-	-	-	-	-	-	-	-0.6 to -1.4 (-1.6 to -2.4)	2 to 100	-	-	19	Lu, Li, Zhang, and Dong (2008)
East Antarctic	Aug. 1995	Aerial, Satellite	Non-Cum.	-	-	-	-	-	-	-	-1.9 to -3.5 (-2.9 to -4.5) [-3.9 to -5.5]	1 to 150	-	-	6	Paget, Worby, and Michael (2001)
Weddell Sea, Antarctic	Dec. 2004	Aerial	Non-Cum.	-	-	-	-	-	–1.9 (-2.9) [-3.9]	–2.0 to –4.0 (-3.0 to -5.0) [-4.0 to -6.0]	-	2 to 120	20	-	130	Steer, Worby, and Heil (2008)
Weddell Sea	Sept.–Oct. 2006	Helicopter	Cum.	-	-	-	-	-	-1.03 to -1.05 (-2.03 to -2.05)	-5.0 to -7.59 (-6.0 to -8.59)	-	2 to 100	40	-	122	Toyota, Haas, and Tamura (2011)
Wilkes Land, East Antarctic	Sept.-Oct. 2007	Helicopter	Cum.						-1.03 to -1.52 (-2.03 to -2.52)	-3.15 to -5.51 (-4.15 to -6.51)	-	2 to 100	20-40		52	
														-		
Wilkes Land, East Antarctic	Sept.–Nov. 2012	Helicopter, Satellite	Cum.	-	-	-	-	-	– 2.9 to –3.1 (-2.9 to -3.1)	–1.3 to –1.4 (-2.3 to -2.4)	-	5 to 10,000	100		16	Toyota, Kohout, and Fraser (2015)
														-		
ARCTIC																ARCTIC
East Siberian Sea	Jun.–Aug. 2000–2002	Satellite	Cum.	–0.3 to –0.6	–0.6 to –1.0	-	30 to 28,400,000	280,000 to 485,000	-	-	-	-	-	78-95	6	Geise, Barton, and Tebbens (2016)
Barents/Kara Seas	Spring 2000, 2001, 2009	Aerial, Satellite	Non-Cum.	-	-	-	-	-	-	-	-2 (-3) [-4]	2 to 5000	-	-	3	Gherardi and Lagomarsino (2015)
Beaufort, Chukchi, and Wrangel Seas	Aug. 1992	Satellite	Cum.	-	-	-	-	-	-	-	–1.9 to –2.6 (-2.9 to -3.6)	1000 to 20,000	-	-	15	Holt and Martin (2001)
Beaufort Sea	May–Sept. 2014	Satellite	Non-Cum.	-	-	-	-	-	-	-	–2.7 to –4.0 (-3.7 to 5.0) [-4.7 to -6.0]	450 to 3000	-	-	4	Hwang and others (2017)
Sea of Okhotsk	Feb. 18, 2000	Aerial	Cum.	-	-	-	-	-	-	-	–1.5 to –2.1 (2.5 to -3.1)	10 to 100	-	-	2	Inoue, Wakatsuchi, and Fujiyoshi (2004)
Sea of Okhotsk	Dec. 1984	Satellite	Cum.	-	-	-	-	-	-	-	–2.2 (-3.2)	5 to 30	-	-	1	Matsushita (1985)
Beaufort Sea	Jun.–Sept. 1998	Aerial, Satellite	Cum.	-	-	-	-	-	-	-	–2.0 to –2.2 (-3.0 to -3.2)	10 to 10,000	-	-	9	Perovich and Jones (2014)
Beaufort Sea	Jun.–Aug. 1973–1975	Aerial, Satellite	Cum.	-	-	-	-	-	-	-	–1.7 to –2.5 (-2.7 to -3.5)	1000 to 20,000	-	-	7	Rothrock and Thorndike (1984)
Beaufort and Chukchi Seas	Mar.–Oct. 2013, 2014	Satellite	Non-Cum.	-	-	-	-	-	-	-	–2.0 to –2.9 (-3.0 to -3.9) [-4.0 to -4.9]	10 to 30,000	-	-	273	Stern, Schweiger, Zhang, and Steele (2018)
Sea of Okhotsk	Feb. 2003	Aerial, Heli, Icebreaker	Cum.	-	-	-	-	-	–1.15 (-2.15)	–1.87 (-2.87)	-	1 to 1500	40	-	4	Toyota, Takatsuji, and Nakayama (2006)
Beaufort and Chukchi Seas	Summer–Fall 2014	Satellite	Cum.	-	-	-	-	-	-	-	-2.77 to -4.12 (-3.77 to -5.12)	1 to 40,000	-	-	18	Wang, Holt, Rogers, Thomson, and Shen (2016)